

NASA Contractor Report 3525

NASA
CR
3525
c.1

Cryogenic Performance of Slotted Brazen René 41 Honeycomb Panels

Andrew K. Hepler and Allan R. Swegle

CONTRACT NAS1-14213
JUNE 1982

FOR COPY: RETURN TO
NASA TECHNICAL LIBRARY
WRIGHT PATER BLDG



NASA

TABLE OF CONTENTS

	<u>PAGE</u>
SUMMARY	1
INTRODUCTION	3
DESCRIPTION OF TEST PANELS	5
Design and Test Conditions	7
FABRICATION OF PANELS	8
SPECIMEN 1 TESTS	10
Test Set Up	10
Test Instrumentation	12
Test Plan	13
Tests	14
SPECIMEN 1 TEST RESULTS	16
Post-Test Inspection	19
RECOMMENDATIONS FOR FUTURE TESTS	22
CONCLUSIONS	23
REFERENCES	25
APPENDIX A - PANEL DESIGN ANALYSIS	49
APPENDIX B - TEST LOG	77

LIST OF FIGURES

<u>NO.</u>	<u>TITLE</u>	<u>PAGE</u>
1	Specimen 1 Inner Surfaces and Honeycomb Core Plan View	26
2	Specimen 1 External Surface Plan View	27
3	Specimen 1 Side View and Bill of Material	28
4	Specimen 2 Plan View	29
5	Specimen 2 Side View	30
6	Specimen 2 Slot Details and Bill of Material	31
7	Specimen 1 External Surface Temperature Cycle	32
8	Specimen 1 Sheet Thickness Before and After Chem-Milling	33
9	Specimen 1 Seal to Test Fixture	34
10	Specimen 2 NASA LaRC High Temperature Structures Wind Tunnel Interface Forward and Aft Edges	35
11	Specimen 2 NASA LaRC High Temperature Structures Interface - Long Side Edges	36
12	Test Area 41 Tulalip Test Site	37
13	Specimen 1 Liquid Hydrogen & Radiant Heat Lamp Test Setup	38
14	Specimen 1 Test Fixture Mounting	39
15	Specimen 1 Thermocouple and Strain Gage Layout	40
16	Specimen 1 Test Plan Summary	41
17	Specimen 1 Maximum & Minimum Inside and Outside Surface Temperatures	42
18	Specimen 1 Frost Formation Forty Minutes After Cool Down Following the Tenth Cycle	43
19	Specimen 1 First Cycle Heat Pulse - K	44
20	Specimen 1 First Cycle Heat Pulse - ⁰ F	45
21	Maximum Thermocouple Readings During Cyclic Exposure See Figure 15 for Thermocouple Locations	46
22	Minimum Thermocouple Readings During Cyclic Exposure See Figure 15 for Thermocouple Locations	47

SUMMARY

This is the final report of a four phase program coordinated under NASA Contract NAS1-14213 to develop selected preliminary mechanical and physical properties for brazed Rene'41 honeycomb sandwich. The objectives of the program were 1) to develop preliminary structural design properties, 2) to assess the effect of cyclic combined thermal and mechanical loads at high strain levels, 3) to determine effective thermal conductivity, and 4) to evaluate the effect of slots in the outer honeycomb face sheet when the sandwich is exposed to cryogenic tankage application or to a hypersonic entry environment representative of that which would be experienced by a space transportation vehicle with a low wing loading. Results of the first three phases have been published. This report covers the fourth phase.

The objective of the fourth phase was to design, fabricate and test two Rene'41 honeycomb panels that simulate the honeycomb lower surface and integral supporting frame structure of an advanced space transportation vehicle. The inner skin of the vehicle's Rene'41 honeycomb surface panels forms the containment for liquid hydrogen and liquid oxygen. The outer skin is slotted to provide thermal stress relief to the skins. Slot covers were provided for some slots. The first panel was subjected to a simulated cyclic thermal boost environment encountered by an advanced space transportation vehicle. The second panel was fabricated for tests by NASA at NASA Langley Research Center's High Temperature Structures Tunnel at temperatures and hypersonic flow conditions to simulate the entry environment imposed on an advanced space transportation vehicle. Discussion of the design conditions and specimen configuration, design analysis data, and fabrication results for both panels are included in this report.

The first specimen was tested to evaluate the performance of the covered and uncovered slots in the outer skin and the adjacent honeycomb core when subjected to extensive frost accumulation and the potential existence of liquid air. Also, the first specimen was used to investigate the effect of thermal stresses in the skins and the core which occur when the radiantly heated outer skin and the LH₂ cooled inner skin are forced to conform to the shape of the relatively stiff integral frame. Specimen 1 testing was terminated by a test setup fire at the conclusion of thirty-six thermal cycles. The specimen completed the test with no structural damage as determined by post-test X-Ray, C-Scan, visual examination and extensive analysis of photomicrographs. Specimen 1 test instrumentation, plan, data, analysis of test data, and recommendations are included in this report.

The second specimen was designed similarly to Specimen 1 and was configured to be tested in the NASA LaRC Eight Foot High Temperature Structures Tunnel (HTST). This test will simulate the aerothermal entry conditions on a low wing loading advanced space transportation vehicle. The test will impose hypersonic aerothermal conditions on the panel external face containing longitudinal running uncovered and covered slots with various spacings and lengths.

INTRODUCTION

This is the final report of a four phase program conducted under NASA Contract 14213 to develop selected brazed Rene'41 honeycomb sandwich preliminary mechanical and physical properties.

The objective of the first phase of the program, reported in Ref. 1, was to develop preliminary mechanical design properties for brazed Rene'41 honeycomb sandwich. Strength data, creep data and residual strength data after cyclic thermal exposure were obtained at temperatures ranging from 78K to 1144K (-320⁰F to 1600⁰F). The influences of face thickness, core depth, core gage, cell size, and thermal/stress exposure conditions on the mechanical design properties were investigated.

The objective of the second phase of the program, reported in Ref. 2, was to design and fabricate large brazed Rene'41 honeycomb panels, to establish a test plan to subject the panels to combined cyclic thermal gradients and mechanical loads equivalent to those imposed on an advanced space transportation vehicle (Ref. 3) during its boost and entry trajectories, and to design and fabricate a test fixture for the cyclic tests. Two Rene'41 brazed honeycomb panels were designed and fabricated. The panels were sized to be subjected to combined cyclic thermal and mechanical loads representative of operating loads for the Ref. 3 vehicle. The panels will be tested to measure and evaluate stresses induced by thermal gradients and mechanical loads. Test conditions include both high thermal and high mechanical loads typical of space vehicle boost conditions for an integral, cryogenic-tank hot structure and moderate thermal and low mechanical loads typical of high temperature entry conditions.

In the third phase of the program, effective thermal conductivities of brazed Rene'41 honeycomb panels were determined analytically and experimentally for temperature ranges between 20.4K (-423⁰F) and 1186K (1675⁰F) and was reported in Ref. 4. The cryogenic data were obtained using a cryostat whereas the high temperature data were obtained in a heat flow meter and a comparative thermal conductivity instrument. Comparisons between experimental data and analysis were developed.

The objective of this fourth phase of the program was to design and fabricate two Rene'41 brazed honeycomb panels that would incorporate a typical integral frame element and to conduct tests that would subject these structures to thermal environments imposed on the Ref. 3 advanced space transportation vehicle during its boost and entry trajectories. The external surface on such a vehicle requires no additional thermal protection. The inside face of the surface panels form the containment for liquid hydrogen (LH₂) and liquid oxygen. Slots were incorporated in the outer surface for thermal stress relief in the surface skins. Slot covers were provided for some slots.

The first panel fabricated in this phase was tested to evaluate the performance of the covered and uncovered slots in the outer skin and the adjacent honeycomb core when subjected to extensive frost accumulation and the potential existence of liquid air. Also, the first specimen was used to investigate the effect of thermal stresses in the skins and the core which occur when the radiantly heated outer skin and the LH₂ cooled inner skin are forced to conform to the shape of the LH₂ cooled and relatively stiff integral frame.

The second panel was designed to be subjected to entry temperature and mass air flow in the NASA LaRC High Temperature Structures Tunnel. This test was designed to evaluate the affects of hypersonic mass flow on open and covered slots. Longitudinal (streamwise) skin stresses adjacent to and between

frames caused by panel differential temperatures will be representative of the Ref. 3 vehicle stresses at peak entry temperatures, and panel transverse stresses due to frame restraint of panel deformations will be realistically imposed.

DESCRIPTION OF TEST PANELS

Specimen 1 was configured to provide two equal spans. A minimum of two spans are required to provide thermally induced moments over the frame and to evaluate the effect of frame restraint on the panel. The length of the spans was determined by an average core shear level requirement. This level was set in the range generated by fuel pressure in the Ref. 3 vehicle. The width of the specimen was determined so that several varied slot spacings in the outer skin could be evaluated during the test. Frame depth was selected from the Ref. 3 vehicle design to provide equivalent lateral and vertical restraint to thermally induced displacements and loads.

Test Specimen 1 is shown in Figures 1, 2 and 3. It was designed to be subjected to liquid hydrogen on its inner face and frame segment while simultaneously being radiantly heated to a temperature of 478K (400⁰F) on the outer face. The specimen was 53.3 cm (21 in.) X 64.8 cm (25.5 in.) X 3.05 cm (1.2 in.) deep. It had a 10.2 cm (4 in.) deep frame running parallel to the 64.8 cm (25.5 in.) dimension and 26.67 cm (10.5 in.) from each long edge. The skins were chem-milled to be thicker near the frame, and core density was increased near the frame because local loads are higher in this region. The Rene'41 honeycomb core was 3.05 cm (1.2 in.) deep and varied from 150.6 kg/m³ (9.4 lb/ft³) to 301.2 kg/m³ (18.8 lb/ft³) density.

Slots were incorporated at various spacing in the outer surface for thermal stress relief in the surface skins. The effects of slot spacing and the length of the slots on relieving thermal stress are discussed in Appendix A. Slots were both covered and uncovered. Slot covers may be required to prevent flow into the honeycomb core during the high heating regimes of the flight. The effects of cryogenic exposure on covered and uncovered slots will be evaluated on Specimen 1. Hastelloy X sheet was welded around the edges of the inner skin to provide an LH₂ seal between the panel and test fixture.

The Specimen 2 panel was configured to the size requirements of the facility holding fixture in terms of length and width dimensions and the spacing of the two panel frames. Skin and core sizing was selected to be similar to the Specimen 1 requirements in order to provide sizing similar to the Ref. 3 vehicle. Test Specimen 2 is shown in Figures 4, 5 and 6. It was designed to be tested in the NASA LaRC 8-Foot High Temperature Structures Tunnel (HTST) to a maximum temperature of 1034K (1400⁰F) on the external surfaces in a Mach 7 airflow. Specimen 2 was 87.1 cm (34.3 in.) X 56.6 cm (22.3 in.) X 3.05 cm (1.2 in.) deep. It had two 10.2 cm (4 in.) deep frames running parallel to the 56.6 cm (22.3 in.) dimension. The first frame was located 26.1 cm (10.28 in.) from the forward edge of the panel and the second frame was located 61 cm (24.02 in.) aft of the forward edge. The panel outer face was slotted in a similar manner as Specimen 1. Two different types of slot covers were employed as shown in Details II and III in Figures 5 and 6. Some of the slots were left uncovered. The effects of flow on covered and uncovered slots will be determined by the test. The braze material and the honeycomb core material and depth are the same as for Specimen 1. The Rene'41 honeycomb core varies from 75.3 kg/m³ (4.7 lb/ft³) to 301.2 kg/m³ (18.8 lb/ft³). Chem-milling of inner and outer skins centered on the two frames

is similar to Specimen 1. Slotted angles overlapping the hot-side face as shown in Figures 4 and 5 were used as edge seals to the test fixture.

Design and Test Conditions

Specimen 1.-The Specimen 1 design load and test condition consisted of a thermal input to the panel which subjected the .038 cm (.015 in.) gage external surface of the panel to 478K (400⁰F) while the inside surface and frame was immersed in nonpressurized liquid hydrogen (LH₂) at a temperature of 20K (-423⁰F). Figure 7 shows the external surface test heat input to the .038 cm (.015 in.) surface. The panel was designed to be exposed to this heating cycle 100 times during the test program while the LH₂ was maintained continuously against the inner skin and frame. The exceptions to the typical cycle were as follows: (1) on the first, ninth and then on each succeeding tenth cycle, the specimen was exposed to the LH₂ for one hour prior to imposing the heat cycle and (2) after the tenth and thirtieth cycle, the LH₂ was purged from the test setup so that the external surface of the specimen could be visually inspected.

The test thermal environments were designed to duplicate the Ref. 3 vehicle ground and boost thermal environments. The one hour holding time for LH₂ exposure was designed to simulate long time ground standby of a fully fueled vehicle ready for an "on-demand" or immediate requirement to launch.

Specimen 2.-The second specimen will be tested in the NASA Langley Research Center (NASA LaRC) 8-Foot High Temperature Structures Tunnel (HTST) under hypersonic flow. The specimen exterior surface will be preheated to a maximum of 1034K (1400⁰F) with radiant heat lamps prior to subjecting the test panel to hypersonic flow. The test panel design requirements state that the interior surface temperature shall not be more than 111K (200⁰F) below that of the exterior surface and the frame will not be more than 167K (300⁰F) below the

exterior surface temperature. The test requirement for differential temperature limitation between surfaces is necessary in order to limit the skin stresses, longitudinal and transverse core shear and normal core loads generated by the test panel end supports to load levels present in the Ref. 3 vehicle at maximum entry temperatures.

The HTST test will simulate the hypersonic flow and the peak reentry temperatures encountered by the Ref. 3 vehicle slotted surface panels.

FABRICATION OF PANELS

Materials and processes specifications and the bill of materials for Specimens 1 and 2 are noted in Figures 3 and 6, respectively. AMI 937 (developed as 930 FOB) braze alloy was used. Braze temperature was 1326.6K (1927⁰F).

Figure 8 shows the sheet thickness at specific locations of Specimen 1 before and after chem-milling. The Rene'41 chem-milled face gages were stepped from .038 cm (.015 in.) to .051 cm (.02 in.) to .071 cm (.028 in.) on the hot side and from .038 cm (.015 in.) to .051 cm (.02 in.) to .064 cm (.025 in.) to .102 cm (.04 in.) on the cold side. The skins were chem-milled after brazing. Slots were cut in the external skin after chem-milling with diamond imbedded wheels the same thickness as the desired slot width.

The panel frames were attached to the panels by a combination of brazing and welding. Tee sections as shown in Figure 3 as part 254-20811-1 were brazed to the panels with 310 gm/m² (.2 gm/IN²) of braze alloy on each faying surface. The tees each had a nib raising to a height of .64 cm (.25 in.) from the panel surface. The frame web was then tungsten inert gas (TIG) welded to the tee nib with Hastelloy W weld wire. The frame web was welded after brazing, chem-milling and slotting of the outer skin.

The initial design of Specimen 1 called for a slot and slot cover and groove similar to the configuration shown in Detail II in Figure 6. The groove was machined into the core prior to brazing. The core was erroneously brazed with the groove against the inner skin with the frame tee (brazed simultaneously) rather than with the groove against the outer skin. The Figure 6 Detail II seal configuration was abandoned for Specimen 1 because of the cost of replacement and a lack of replacement core. The gap between the inner skin and core caused by the groove was left as-is since that unstabilized section of skin is normally exposed to only tension stresses. The abandoned groove is shown in Figure 15.

Slot covers were welded to the outer skin after the frame webs were welded to the tees. The Specimen 1 -14 slot cover shown on the right side of Figure 2 was condenser discharge welded to the panel. The other Specimen 1 slot covers were electron beam (EB) welded to the panel after first being tacked to the panel by condenser discharge welding. All Specimen 2 slot covers were condenser discharge welded to the panel to save cost and because of the more satisfactory results of this type of welding at the present level of development. The outer skin chem-milled pads were shaped to allow the slot covers to weld flat to a uniform sheet thickness in the same plane.

A Hastelloy X .038 cm (.015 in.) picture framed shaped sheet as shown in Figure 9 was EB welded to the edges of Specimen 1 after being initially tacked to the panel by condenser discharge welding. The Hastelloy X sheet provided a flexible seal between the specimen and the test fixture. A .16 cm (.063 in.) 321 stainless steel picture frame shaped strip shown in Figure 9 was seam welded to the outer edges of the Hastelloy X seal to provide the material to be (TIG) welded to the .16 cm (.063 in.) gage lip of the LH₂ container.

Specimen 2 panel edge seals to the test facility consisted of .038 cm (.015 in.) gage slotted angles shown in Figures 5, 10 and 11. The angles were condenser discharge welded to the panel.

SPECIMEN 1 TESTS

Test Set Up

Specimen 1 was tested at Boeing's Tulalip Test Site located 19 Km (12 miles) North of Everett, Washington. The Tulalip Test Site provides many remote test pads, facilities and equipment which can be used for hazardous tests.

The overall Specimen 1 test site is shown in Figure 12. Figure 12 schematically illustrates the Area 41, Pad 1 location of the test setup and its relationship to the instrumentation readout control room, LH₂ dewar and supply lines and gaseous helium and liquid nitrogen storage. Area 41 is located in a 152 m (500 ft) diameter clearing surrounded by dense second growth forest that is approximately .8 Km (.5 miles) from the closest test facility.

The test setup is shown in Figure 13. This figure shows the foam insulated LH₂ cryostat, its support structure and the 7.62 cm (3 in.) deep foam insulated lid which is restrained by metal straps pretensioned by bungee cords. The hydrogen fill, purge and vent lines are accessed through the cryostat lid. Figure 13 also shows the radiant heat lamps that supply the simulated boost trajectory heat input.

The support of Specimen 1 by the test fixture panel support frame is displayed in Figure 14. The long edge of Specimen 1 bears on a rigidized fiberfrax pad on the support frame. The Specimen 1 integral frame is tied to the same test fixture support frame by a pretest adjusted bolt at each end

of the panel frame which, with panel end bearing, provides restraint to vertical displacement. The test fixture panel support frame is totally immersed in LH₂ during the test except during periods when the LH₂ container is purged.

LH₂ pressure was purposely maintained at or near ambient pressure by means of the 10.2 cm (4 in.) diameter vent stack and by the natural leakage of boil-off of hydrogen gas at the lid lip. Insulation of the container and lid were provided by the use of 7.62 cm (3 in.) of Lastafoam applied between wooden forms (later removed) and the LH₂ container. It was recognized that this particular test fixture design was inferior in both life and fire safety to a valve-vented, pressure-sealed, and vacuum-jacket-insulated design. The higher pressure test setup would have exceeded the allowable contract costs. The test hazards were thought to be minimal for the unsealed, foam insulated design with respect to the test specimen and were not significant to personnel safety because of the remote test site and no personnel access beyond the control room during LH₂ loading and test. The possibly short life of the foam due to separation from the container or internal cracking during cyclic purging was accepted as a life cycle limiter in order to achieve major test cost savings.

The radiant heat lamp bank consisted of fifteen gold-plated reflectors with eight 1000 watt quartz bulbs (1000T3-CL-HT-240V) in each reflector. The reflectors were wired as five parallel circuits with each circuit containing three reflectors wired in series.

The panel temperature was monitored and lamp power was regulated with a Data Trak Controller (Model #73211, Boeing #10225573). The Data Trak Controller monitored the panel thermocouple output, compared it to the programmed thermal cycle, and by adjusting the lamp power, eliminated the error between the signals.

The power unit was a 480 V three phase, two channel unit with six controllers (Boeing #10225831). Only Controller #1 was used, and it was used in the automatic mode (automatic mode slaved the power controller to the Data Trak Controller). The power unit and controller were supplied to Boeing as a complete system by Research Inc. (Model 202524).

A Fluke data logger (Model 2240B, Boeing #BC 576451) was used to record all data other than monitor data. The data were printed on a 5.6 cm (2.2 in.) paper tape.

The test was continuously monitored with a remote control infrared T. V. camera. The camera had pan, tilt, zoom and focus capabilities.

Photos of the specimen were also taken. These included stills and motion pictures. The stills were shot before and after testing to show setup, specimen conditions and cryostat conditions. Both quasi-real time (8 frames a second) and time lapse (a frame every 6 seconds) were taken during the test. The time lapse camera ran for the entire test while the real time camera was used to record the frost formation during the first hold and the first heat cycle.

Test Instrumentation

Specimen 1 instrumentation included twenty-two thermocouples (T/C) and four strain gages. The originally applied tri-axial strain gages (Micro-Measurements WK-06-060WR-350) were shorted during the welding of the test specimen seal to the LH₂ container due to improper grounding. Micro-Measurements WA-06-120WR-350 tri-axial strain gages were substituted as replacement gages. The substitution was not discovered until test setup installation was complete and instrumentation calibration was in progress. Micro-Measurements data indicated that short time exposure to 77K (-320⁰F) would not harm the gages, and the substitution was considered acceptable.

However, the gages provided erratic and useless data after initial exposure to temperatures of 200K (-100°F).

The location of the twenty external surface T/C and two internal surface T/C are also shown in Figure 15. T/C 15 on the inside surface and T/C 18 adjacent to the controller T/C 17 on the outside surface were routed to strip chart recorders. T/C 16 was used as a limiter to cutoff heat input if outer surfaces should exceed 5054K (450°F). The thermocouple leads were extended from the reference junction and, except for the four gages mentioned above, were fed directly into the data logger.

Single pressure gages monitored the LH₂ dewar pressure, transport line pressure and LH₂ container pressure. The LH₂ level in the container was monitored and automatically controlled by using Boeing designed carbon resistors. The resistors caused the LH₂ to fill the container when the LH₂ fell to a minimum level and to shutoff when it reached the peak level.

Test Plan

The Specimen 1 test plan is summarized in Figure 16. The test was conducted in groups of repeating 10 cycles featuring the cool down, stabilization and hold on the first cycle which amounted to a one hour hold with some variable tolerance for test control purposes under LH₂ only exposure. Then the thermal cycle shown in Figure 7 was imposed. The cycle contained a 90 second hold at the peak temperature of 478K (400°F). Following cool down, temperatures were stabilized under LH₂ exposure and held for 10 minutes, after which the thermal cycle was repeated. At the conclusion of the ninth cycle cool down, the LH₂ exposure was held one hour after low temperature stabilization. After this one hour hold, the tenth cycle thermal cycle was conducted.

Following the thermal cycles of the tenth, thirtieth and fiftieth cycles, visual inspections were to be conducted after the LH₂ container was purged of LH₂. The test was to be terminated at the completion of 100 cycles.

Tests

The Specimen 1 test started on October 14, 1980 at 10:00 a.m. High and low T/C readings for T/C 14 on .038 cm (.015 in.) gage material on the external surface and for T/C 8 on the internal surface are shown for each of the test cycles in Figure 17. These values can be compared with Appendix A, Figure A-5 which shows the outside surface temperature values used for the computer analysis for the theoretically desired temperatures. A temperature overshoot to as high as 683K (770⁰F) occurred on the first cycle. It is possible that frost formation on the cluster of T/C's near the control T/C caused the heat lamps to drive the frost free areas to the high values shown on the first cycle. A different T/C was selected as a control for the heat lamps and the remainder of the cycles were satisfactorily controlled.

Strain gage readings became erratic when temperatures dropped below the 222 to 199K (-60 to -100⁰F) range during the first cycle and remained so during the remainder of the test.

Panel visual inspections of the outside surface were conducted at the end of 10 and 30 cycles. The panel remained smooth and flat. Coin tapping of the external surface revealed no unusual sounds. The slot covers and the open slots showed no unusual signs during the inspections.

Frost buildup during LH₂ only exposure could be readily followed. The panel external surface was monitored continuously with a controllable zoom lens. It was particularly noticeable along covered and uncovered slots. Strain gage wires seemed to attract frost buildup and icicle like formations.

Figure 18, taken from 16 mm movie film used for the time lapse photography, shows a typical frost buildup late in the fifty-five minute cool down following cycle ten with outer surface temperatures steady at approximately 150K (-190°F). The area mentioned in the fabrication section as having a .79 wide by .11 by 53.3 cm long (.31 X .045 X 21 inches) groove in the core, brazed in error against the inside surface, attracted frost to the point of apparently building up an ice coating. The frost on this zone apparently partially melted during each relatively brief heating cycle to form an ice layer on the external surface. Because this groove was open to the air on each end of the panel, it probably contained liquid air during the cooler portions of the cycle and probably retained enough cold air in the honeycomb core under the external skin to keep that skin locally cold.

An ice layer seemed to build during the course of cyclic cooling and heating on a narrow strip of external surface in the densified core area adjacent to the panels internal frame. The initial cooling cycle (representative of a vehicle operation) appeared to build only frost on the external panel surface.

The test specimen of course did not have the boost aerodynamic surface forces or the normal vibration/acoustic affects of vehicle operation that could be expected to accelerate frost removal. All frost/ice was melted during the purge of LH₂ test container preceeding the inspections.

Flames appeared around the upper areas near the lid of the insulated LH₂ container following the cool down of cycle 36. Several small pieces of the foam insulation blew away from the outside of the LH₂ container. No explosion was seen or heard. The fire was extinguished with the gradual introduction of the purging inert gases. The external insulation on the container was burned, but the test specimen and the liquid hydrogen metal container were not damaged. A condensation of the test log is given in Appendix B.

SPECIMEN 1 TEST RESULTS

The panel sustained a severe temperature pulse on the first heating cycle. Figure 19 and 20 shows the range of temperatures from just before the heat pulse to several minutes into the subsequent cold stabilization period following panel heating. The maximum temperatures were attained at 11:33:20 a.m. with a maximum recorded reading of 682K (768⁰F) on T/C 3. The desired temperature was 477K (400⁰F) at the T/C 3 location. A narrow zone along the frame centerline and between the slots approached 533K (500⁰F), which was approximately 108K (195⁰F) above the anticipated temperature. Most areas with .038 cm (.015 in.) gage sheet had zones between slots that attained temperatures in excess of 644K (700⁰F).

As noted previously, the strain gages did not function properly during the test. Test stresses occurring during peak heating of the first cycle were conservatively estimated by comparing calculated test thermal moments derived from average test skin temperatures across each zone skin gage to the calculated moments based on expected temperatures and FEM gages and to the stresses determined by FEM analysis. The overshoot temperatures on cycle 1 were developed in a transient situation which apparently produced high temperature gradients emanating from skin slots and unsealed core splices. The temperatures in areas involving .046 cm (.018 in.) gage outer skins attained an average temperature of at least 542K (515⁰F) rather than the 400⁰F planned. The temperature over the spar was estimated to average 453K (356⁰F) instead of the anticipated 425K (305⁰F). Areas covered by the .060 cm (.0235 in.) gage skin attained an estimated average temperature of 474K (393⁰F) rather than the expected 478K (400⁰F). Using actual skin gages as shown in Figure 8 and actual temperatures, the estimated test thermal moment was increased at least 7% over the moment using actual skin gages and design temperatures. This same percentage increase in

skin, longitudinal core shear and core normal loads should result. Comparisons to FEM analysis of skin stresses should take into account skin thickness differences of the FEM vs. actual skin gages. The peak longitudinal (X-direction) compression stress over the frame probably attained at least 110,000 psi at a peak temperature of 533K (500⁰F). The test transverse core shear stresses at the frame were probably at least 8% higher than those determined by the FEM analysis.

The actual test stress levels may have been higher than noted above because the post test analysis assumed cool zones and steep thermal gradients associated with all specimen edges, outer skin slots, core splices and the .79 cm (.31 in.) groove in the core. These analysis assumptions yield an estimate that the 15.5 cm (6.1 in.) of .046 cm (.018) outer skin on each side of the frame center-line averaged 541K (515⁰F) even though a peak temperature of 679K (762⁰F) was measured. This average temperature estimate may be low by up to 55K (100⁰F).

The slots provided a cooling effect to the adjacent outer skins. The recorded temperatures adjacent to the slots varied widely. The variations indicate that the local condition of the honeycomb core (vacuum sealed or unsealed cells) was significant to the temperature variation. The temperatures measured by T/C's 5, 7 and 9, each located .64 cm (.25 in.) from slots, but each recording significantly different temperatures, illustrate this effect.

The .79 cm (.31) wide groove in the core against the inner skin, previously mentioned, apparently provided a source for supply of liquid air and had a significant cooling effect on a local zone running through the center of the panel parallel to the 53.3 cm (21 in.) dimension. Closed circuit T-V during the test as well as test motion pictures showed that a band of frost or ice at this zone was maintained during repeated heating cycles.

The core splices (see Figures 1 and 2) at 2.03 cm (.8 in.), 5.56 cm (2.2 in.) and at 23.11 cm (9.1 in.) from the frame centerline probably acted as conduits for air. These splices were not seam welded and therefore could not maintain the vacuum in the core in the adjacent cells generally provided to most of the cells by the brazing process. The evacuated core provided better insulation than nonevacuated core. Ice retention in the areas bounded by these splices and over the frame centerline was evident in the motion pictures. The higher conductivity of the higher density core in this local region was a possible contributing cause to ice retention.

The maximum readings of selected T/C's during cyclic thermal exposure are displayed in Figure 21. The minimum readings of the same T/C's are shown in Figure 22. Readings of 88K (-300⁰F) or less may indicate the presence of liquid air.

Thermocouples 5, 7 and 9 were located adjacent to slots. T/C 5 as shown in Figure 22 consistently showed minimum readings below 88K (-300⁰F) and T/C 9 showed the same minimum readings and then on later cycles showed higher minimum readings mixed with cycles of the lower minimums before settling into consistent minimum readings. T/C 7 showed readings lower than 88K (-300⁰F) on two cycles and then returned to higher minimum readings.

Thermocouples 6 and 10 were located .51 cm (.2 in.) from the panel and frame centerline and 1.52 cm (.6 in.) from a core splice. T/C 10 was located 3.81 cm (1.5 in.) from two outer skin slots and T/C 6 was located 7.62 cm (3 in.) from two slots. T/C 10 measured a minimum temperature less than 88K (-300⁰F), then recorded higher minimums before finally consistently recording the lower minimums. T/C 6 recorded higher readings, then later recorded less than 88K (-300⁰F) on two cycles and then recorded higher readings consistently.

Thermocouple 11 was located .51 cm (.2 in.) from a splice and 2.54 cm (1.0 in.) from a outer skin slot. T/C 11 behaved similarly to T/C 6 except that its minimum temperature fell below 88K (-300⁰F) on only 1 cycle, which coincided with the first cycle that T/C 6 fell to that low minimum.

Prior to each heating cycle, the outer skin interfacing with vacuum sealed honeycomb cells and with the container filled with LH₂ should have attained an equilibrium temperature of approximately 144K (-200⁰F). It is probable that outer skin temperatures recording less than 88K (-300⁰F) indicated the presence of liquid air in the adjacent honeycomb cells. It is possible that the cyclic heating and cooling pumped some air to and from incompletely sealed honeycomb cells, thus causing some cells to change minimum temperature readings. All of the T/C's that recorded consistent or occassional minimum readings below 88K (-300⁰F) were within 1.52 cm (.6 in.) of a core splice or an outer skin slot.

Post-Test Inspection

X-rays and C-scans showed no core to skin discontinuities or core buckling phenomena. When the panel was saw cut for metallurgical examination, at selected locations, it was revealed that several void areas were present between the brazed on stiffener (Part No. 254-20811-1, see Figure 3) and the inner skin. X-rays and C-scan had not indicated the presence of the stiffener to skin voids. It was apparent from the undisturbed surface of the braze alloy on the faying surfaces that a braze joint was never accomplished in these void areas. The largest stiffener to skin void area discovered was 3.81 cm (1.5 in.) long and covered the width of the stiffener. Two other smaller void areas covered up to 1.8 cm (0.7 in.) long but less than the full width of the stiffener. Nevertheless, sufficient brazing had taken place between the stiffener and the inner

skin to provide shear and tension strength in the braze joint to meet all the test requirements including the welding of the .18 cm (.070 in.) gage web to the stiffener upstanding rib.

Photomicrographs showed .051 to .076 cm (.02 to .03 in.) honeycomb-to-skin braze fillet sizes compared to a desired size of .076 cm (.03 in.). Core node seam welding must come within .36 cm (.14 in.) of top and bottom surfaces, but must come no closer than .20 cm (.08 in.) to insure core evacuation during the brazing process. Braze node flow of .38 cm (.15 in.) is required to guarantee sealing the top and bottom edges of the honeycomb core. Braze node flow from top and bottom faces ranged from .23 to .36 cm (.089 to .14 in.) in the .32 cm (1/8 in.) cell size core to .30 to .38 cm (.12 to .15 in.) in the .64 cm (1/4 in.) cell size core. Consequently, most but not all cells were sealed.

The photomicrographs and extensive cuts into the panel showed no signs of shear buckling or test-induced core or core/skin braze failure. Two of twenty-four 100X photomicrographs (two each from top and bottom of the core at six locations) showed internal braze fillet cracks not previously seen in photomicrographs from previous test specimens. The other photomicrographs at each of these two locations showed no cracking. Those showing the braze fillet cracks were on the bottom or LH₂ side of the panel. One photomicrograph showed a braze fillet crack appearing adjacent to T/C 14 where overheating of 201K (362⁰F) above the required temperature occurred during the first cycle and in an area otherwise incurring core shear stresses well within the allowable. The second photomicrograph showed a crack within each side of the fillet adjacent to T/C 6 where overheating of 106K (190⁰F) above the required temperature occurred during the first cycle in an area of moderately high shear stress, but also well within the estimated allowable. The two mounts showing cracks appeared to be isolated and did not show on photomicrographs taken of mounts cut

from immediately adjacent areas. Unfortunately all of the mounts were made from specimens that were rough cut with a band saw rather than an abrasive wheel. The band saw is not used for cutting brazed Rene'41 honeycomb in manufacturing work because it tends to rip the skins from the core. The cracks are mentioned in the event future testing reveals a similar cracking. In any event, the cracks were not part of a general failure and did not show at locations where core shear stresses theoretically were at much higher levels. It is not possible to determine when the cracks occurred.

RECOMMENDATIONS FOR FUTURE TESTS

1. Additional testing of high density Rene'41 honeycomb core is required to obtain shear modulus and unidirectional ultimate core shear and core crushing strength and combined longitudinal and transverse shear and core normal stress allowables.

2. Dynamometer bars should be used to measure the reaction loads in future tests of this type. Thermal environment induces thermal strain which may not produce the reaction loads or thermal stresses theoretically described. In the case of this particular specimen configuration, the locally cold areas near the slots and core splices may have produced both skin stress and reaction load relief. Any relief caused by the cooling adjacent to the slots could be taken advantage of in vehicle assessment and sizing.

3. Vacuum jacketing of the LH₂ container while considerably more expensive than the foam insulated, clamp sealed container used, is necessary for long term cyclic exposure or even short term cyclic exposures requiring multiple shutdowns for inspection.

CONCLUSIONS

A two span brazed Rene'41 honeycomb panel with frame, representative of an integral cryogenic tank/fuselage structure was fabricated and exposed to LH₂ and temperature to produce a thermally induced moment and shear loads representative of boost conditions for the space transportation vehicle studied in Ref. 3. The presence of liquid air was probable in certain honeycomb cells near some outer skin slots and core splices as evidenced by outer skin temperature measurements of less than 88K (-300⁰F) during cold hold periods. The core splices between cores of different densities should have been welded continuously at node junctions and improved braze node flow should be developed to provide sealed core along splices and at outer skin slots. There was no evidence of damage to core adjacent to slots where core shear stresses peaked and it may be assumed that the probable presence of liquid air caused no damage to core.

The panel sustained a severe temperature overshoot by as much as 206K (370⁰F) during the first simulated boost thermal cycle. The overshoot caused an increase in skin and core stresses beyond the levels expected. Stresses were not measured, but post-test calculations indicate the peak compression skin stresses reached at least 758 MPA (110,000 psi) at 533K (500⁰F) at the frame centerline. Typical Rene'41 proportional limit and yield stress levels are 607 MPA (88,000 psi) and 827 MPA (120,000 psi) respectively at that temperature. The longitudinal core shear stresses and core normal stresses were probably increased at least 7% and the transverse core shear stresses 8% at the frame centerline compared to finite element analysis.

A strict stress analysis of the finite element analysis loads and the additional loads induced by the temperature overshoot on cycle 1 would indicate

that very localized areas of core might be subjected to failure stresses caused by combinations of longitudinal, transverse and core normal stresses near slots over the frame centerline. The fact that core failure did not occur after 36 cycles of thermal exposures may be attributed to several factors including:

- 1) the areas of high stress are very localized within a 1.27 cm (.5 in.) radius from a slot at the frame centerline and load redistribution from the highly stressed to surrounding core cells probably occurs;
- 2) a secant modulus effect prevails in the highly stressed core that limits the buildup of transverse loads and further aids in load redistribution;
- 3) loads and thermal moments are reduced by plastic deformation of the skin over the frame.

Post-test photomicrographs identified braze fillet cracks in two of twenty-four photomicrographs that did not show in additional photomicrographs taken at these same two widely separated locations. It is not known if the cracks were the result of the first cycle exposure, the total of 36 exposures, or of erroneously being band sawed in making the mount specimens. The specimen showed no signs of structural failure after 36 cycles of thermal exposures. The test showed that a slotted outer skin honeycomb core sandwich fixed integrally to inner frames can withstand thermal strains induced by the localized thermal environment imposed by the Reference 3 vehicle boost trajectory.

A panel was fabricated and delivered to NASA for tests to evaluate the effect of slots in the outer skin, when the panel is exposed to an aerothermal environment.

REFERENCES

1. Hepler, A. K., et al: "Design Data for Brazed Rene'41 Honeycomb Sandwich". NASA Contractor Report 3382, Boeing Aerospace Company, 1981.
2. Hepler, A. K., and Swegle, A. R.: "Design and Fabrication of Brazed Rene'41 Honeycomb Sandwich Structural Panels for Advanced Space Transportation Systems". NASA Contractor Report 165801, Boeing Aerospace Company, 1981.
3. Hepler, A. K., and Bangsund, E. L.: "Technology Requirements for Advanced Earth Orbital Transportation Systems". NASA Contractor Report 2879, Boeing Aerospace Company, 1977.
4. Deriugin, V.: "Thermal Conductivity of Rene'41 Honeycomb Panels". NASA Contractor Report 159367, Boeing Aerospace Company, 1981.

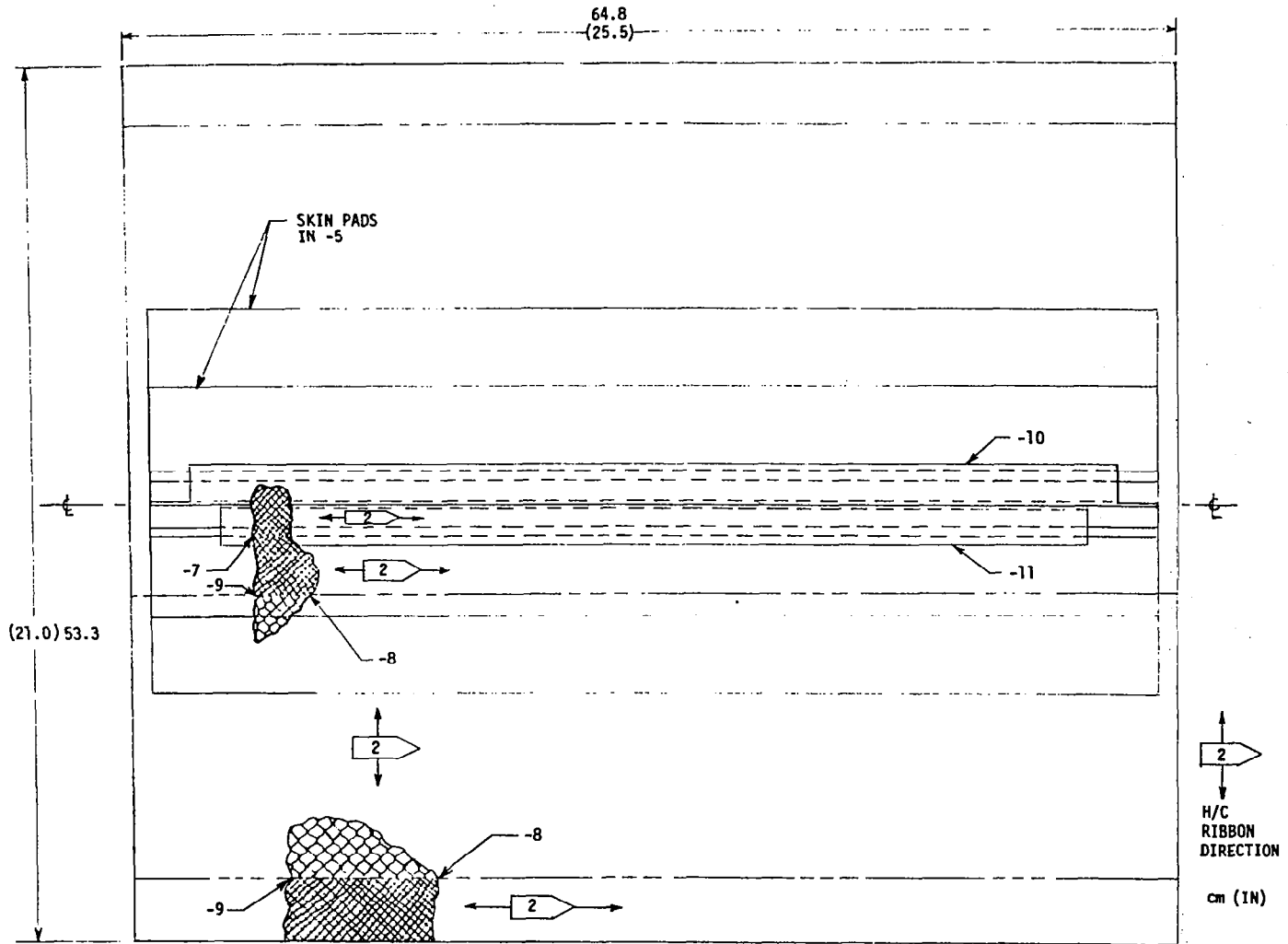


Figure I. Specimen I Inner Surfaces and Honeycomb Core Plan View

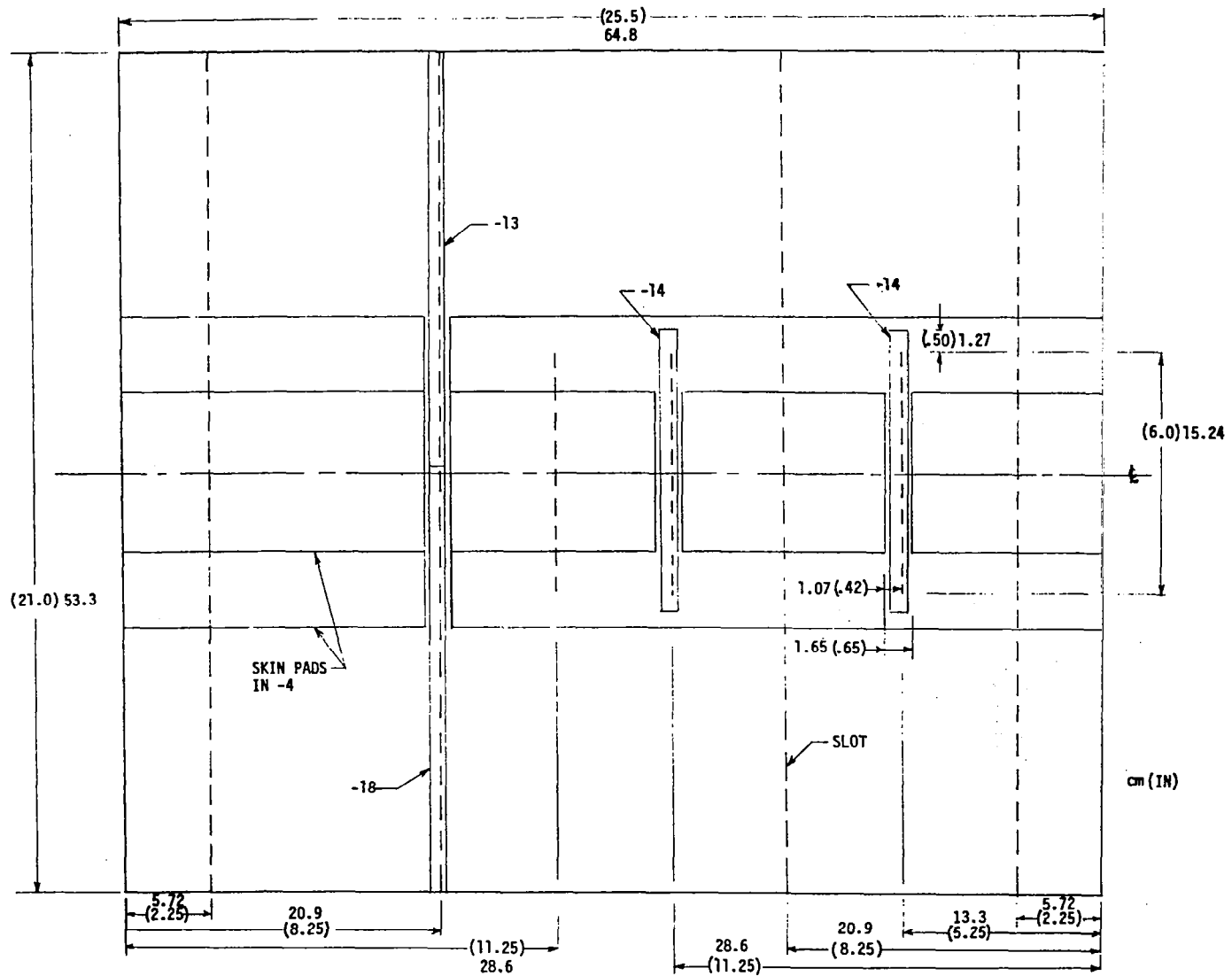
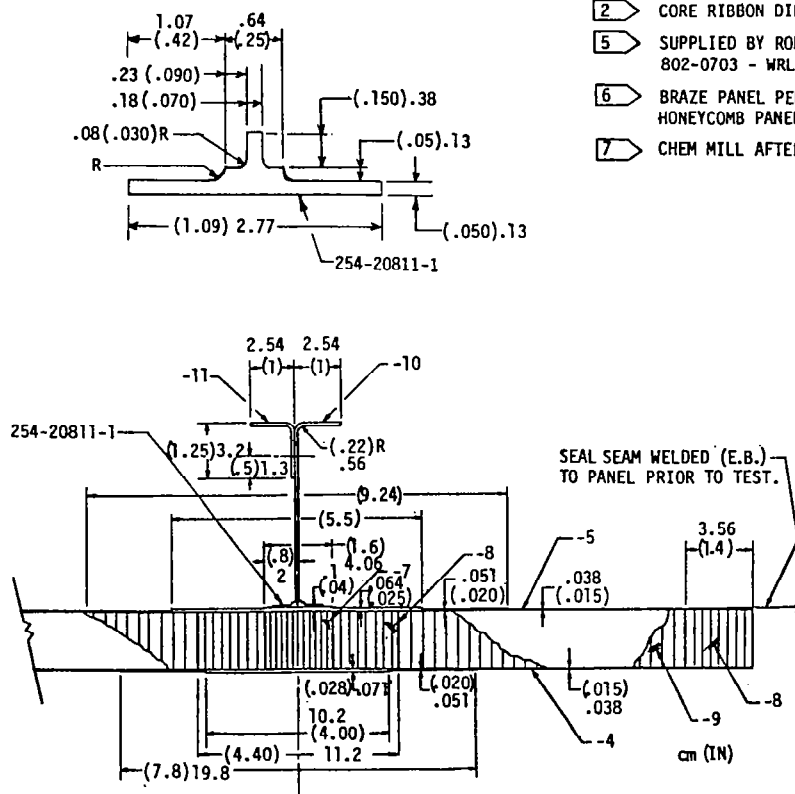


Figure 2. Specimen 1 External Surface Plan View



- 2 CORE RIBBON DIRECTION
- 3 WELD
- 4 SUPPLIED BY BOEING ENGINEERING
- 5 SUPPLIED BY ROHR TO RMS 110 CORE TO BE WELDED PER ROHR MEMO 802-0703 - WRL DATED FEB. 14, 1978 TO BOEING AEROSPACE COMPANY
- 6 BRAZE PANEL PER BOEING PROCESS SPEC VACUUM BRAZING LIGHTWEIGHT RENE'41 HONEYCOMB PANELS - RODNEY FOIL EXCEPT BRAZING TEMP. TO BE REDUCED TO 1325K (1925°F)
- 7 CHEM MILL AFTER BRAZING TOL ± .0051 (.002)

	1	-18	COVER	(.010) X (.50) X (10.8) RENE'41 .025 X 1.27 X 27.4	4
	1	-17(OPP)	ANGLE		
	1	-16	ANGLE		
	1	254-20811-1	CAP		
	2	-14	COVER	(.010) X (.50) X (7.0) RENE'41 .025 X 1.27 X 17.8	4
	1	-13	COVER	(.010) X (.50) X (10.2) RENE'41 .025 X 1.27 X 25.9	4
	1	-11	ANGLE	(.07) X (2.25) X (21.0) RENE'41 .18 X 5.72 X 53.3	4
	1	-10	WEB	(.07) X (5.0) X (25.5) RENE'41 .18 X 12.7 X 64.8	4
	2	-9	CORE	RCBN 4-20 RENE'41 HONEYCOMB CORE (1.20) HIGH X (6.90) X (25.5) 3.05 X 17.5 X 64.8	5
	4	-8	CORE	RCBN 2-15 RENE'41 HONEYCOMB CORE (1.20) HIGH X (1.40) X (25.5) 3.05 X 3.56 X 64.8	5
	1	-7	CORE	RCBN 2-20 RENE'41 HONEYCOMB CORE (1.20) HIGH X (1.60) X (25.5) 3.05 X 4.064 X 64.8	5
	1	-5	SKIN- INNER	(.040) X (21.0) X (25.5) RENE'41 .10 X 53.3 X 64.8	4
	1	-4	SKIN- OUTER	(.040) X (21.0) X (25.5) RENE'41 .10 X 53.3 X 64.8	4
	1	-2	PANEL BRAZE ASSY		6
		-1	PANEL WELD ASSY		
	QTY REQD	QTY REQD	PART NUMBER	NOMEN- CLA- TURE	MATERIAL AND SPECIFICATION
	-2	-1			

Figure 3. Specimen 1 Side View and Bill of Material

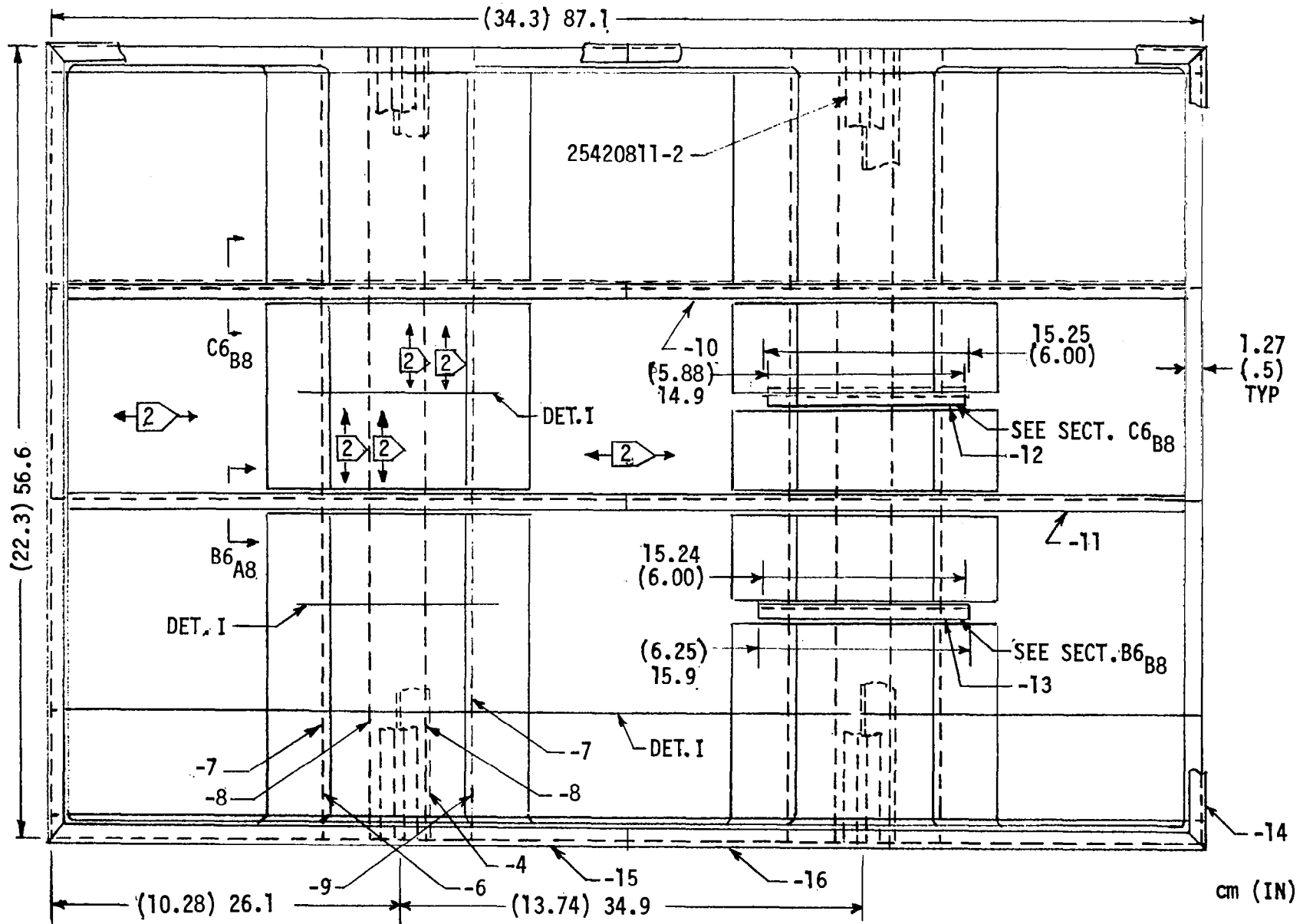


Figure 4. Specimen 2 Plan View

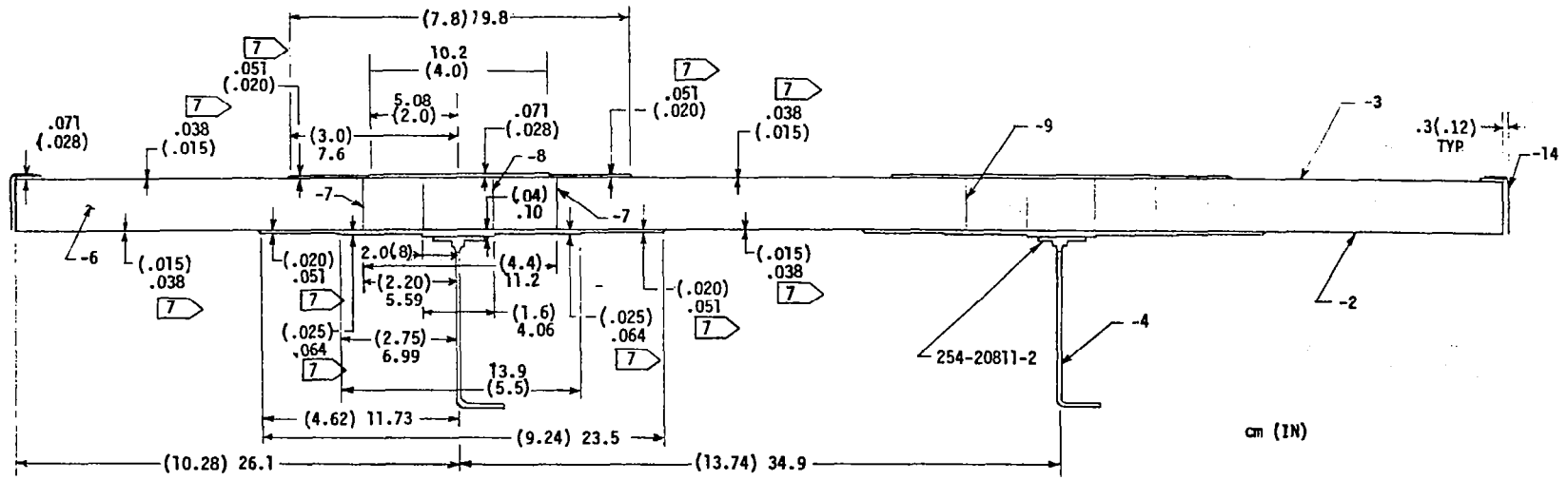
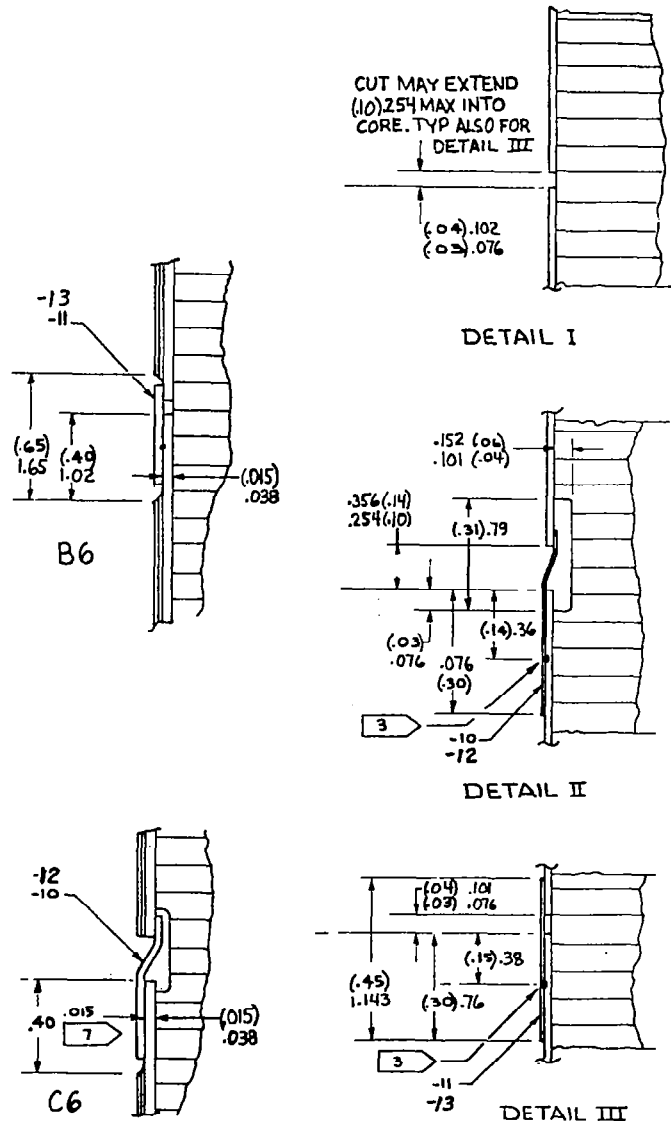


Figure 5. Specimen 2 Side View



- 2 CORE RIBBON DIRECTION
- 3 WELD
- 4 SUPPLIED BY ENGINEERING (BOEING)
- 5 SUPPLIED BY ROHR TO RMS 110 CORE TO BE WELDED PER ROHR. MEMO 802-0703 - WRL DATED FEB. 14, 1978 TO BOEING AEROSPACE CO.
- 6 BRAZE PANELS PER BOEING PROCESS SPEC - VACUUM BRAZING LIGHTWEIGHT RENE'41 HONEYCOMB PANELS - RODNEY FOIL EXCEPT BRAZING TEMP TO BE REDUCED TO 1326K (1925°F)
- 7 CHEM MILL AFTER BRAZING. TOL ± .0051 (.002)
- 8 MEASURE PANEL THICKNESS IN SEVERAL LOCATIONS PRIOR TO BRAZE TO FACILITATE 7

		-17	PANEL ASSY. WELD	
2	-16	EDGE SEAL	.038 X 4.37 X 43.9 (.015) X (1.72) X (17.27) RENE'41	4
2	-15	EDGE SEAL	.038 X 4.37 X 43.9 (.015) X (1.72) X (17.27) RENE'41	4
2	-14	EDGE SEAL	.038 X 4.57 X 57.3 (.015) X (1.80) X (22.54) RENE'41	4
1	-13	COVER	.025 X 1.3 X 15.9 (.010) X (.50) X (6.25) RENE'41	4
1	-12	COVER	.025 X 1.5 X 14.9 (.010) X (.60) X (5.88) RENE'41	4
2	254-20811-2	CAP		
2	-11	SLOT COVER	.025 X 1.3 X 42.1 (.010) X (.50) X (16.58) RENE'41	4
2	-10	SLOT COVER	.025 X 1.5 X 42.1 (.010) X (.60) X (16.58) RENE'41	4
1	-9	CORE	RCB N 6-20 RENE'41 HONEYCOMB CORE 3.05 X 23.7 X 56.6 (1.20) HIGH X (9.34) X (22.3)	5
2	-8	CORE	RCB N2-20 RENE'41 HONEYCOMB CORE 3.05 X 4.06 X 56.6 (1.20) HIGH X (1.60) X (22.3)	5
4	-7	CORE	RCB N2-15 RENE'41 HONEYCOMB CORE 3.05 X 3.56 X 56.6 (1.20) HIGH X (1.40) X (22.3)	5
2	-6	CORE	RCB N6-15 RENE'41 HONEYCOMB CORE 3.05 X 20.52 X 56.6 (1.20) HIGH X (8.08) X (22.3)	5
2	-4	BEAM WEB	.152 X 12.7 X 87.1 (.060) X (5.0) X (34.3) RENE'41	4
1	-3	OUTER SKIN 8	.102 X 56.6 X 87.1 (.040) X (22.3) X (34.3) RENE'41	4
1	-2	INNER SKIN 8	.102 X 56.6 X 87.1 (.040) X (22.3) X (34.3) RENE'41	4
1	-1	PANEL ASSY. HONEYCOMB		6
QTY	QTY	PART	NOMENCLATURE	MATERIAL AND SPECIFICATION
-17	-1			

Figure 6. Specimen 2 Slot Details and Bill of Materials

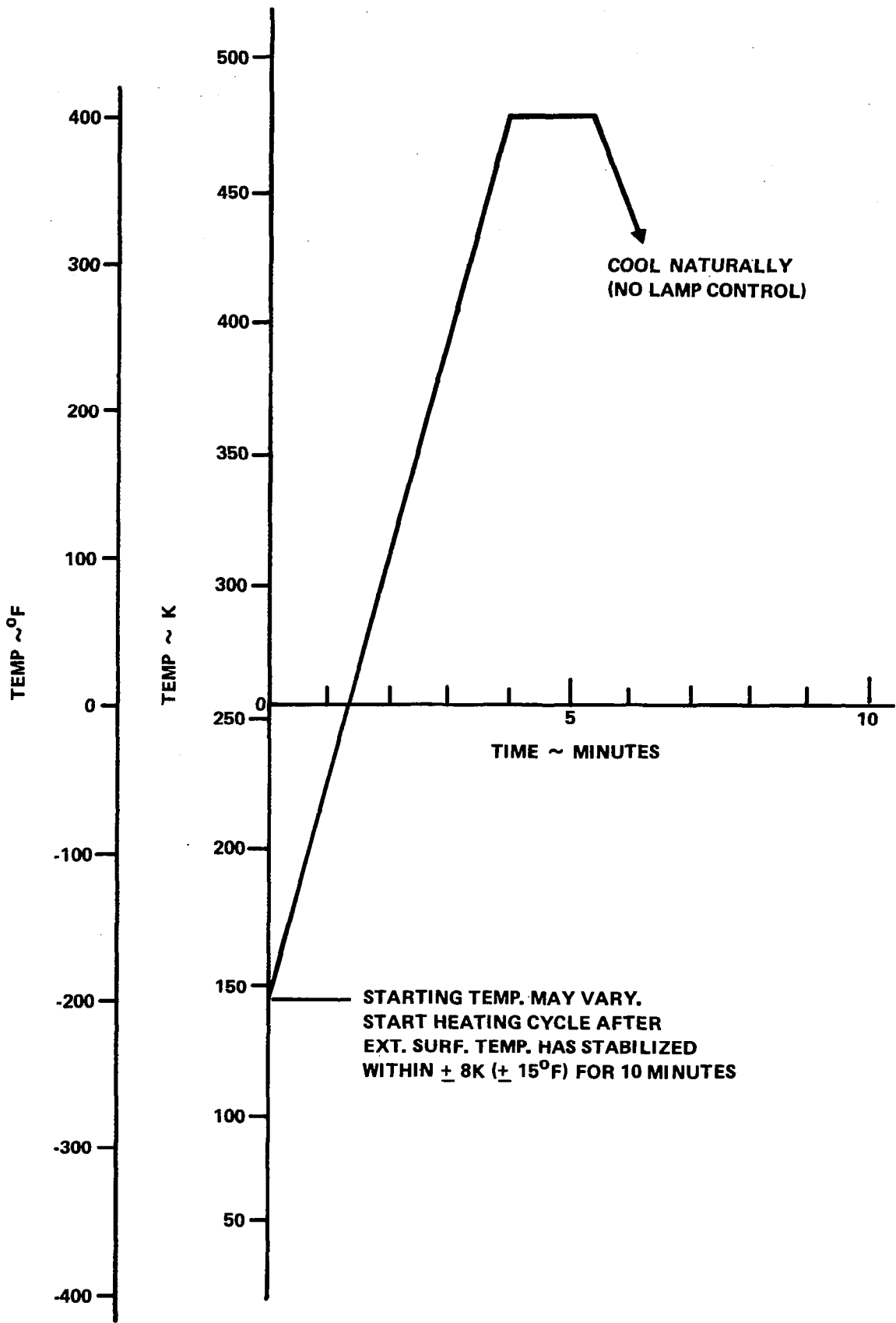




Figure 7. Specimen 1 External Surface Temperature Cycle

SHEET THICKNESS LOCATION	SHEET THICKNESS~CM (IN)					
	BEFORE CHEM-MILLING		AFTER CHEM-MILLING		DRAWING CALLOUT 	
(ADJACENT T/C )	TOP	BOT	TOP	BOT	TOP	BOT
5	.107(.042)	.104(.041)	.107(.042)	.074(.029)	.102(.040)	.071(.028)
6	.107(.042)	.104(.041)	.107(.042)	.072(.0285)	.102(.040)	.071(.028)
10	.107(.042)	.104(.041)	.107(.042)	.072(.0285)	.102(.040)	.071(.028)
11	.107(.042)	.104(.041)	.107(.042) * .069(.027)	.075(.0295)	.102(.040) * .064(.025)	.071(.028)
12	.107(.042)	.104(.041)	.053(.021)	.060(.0235)	.051(.020)	.051(.020)
14	.107(.042)	.104(.041)	.041(.016)	.047(.018)	.038(.015)	.038(.015)

 REF FIGURE 15

 REF. FIGURE 3

* TWO VALUES GIVEN BECAUSE OF CHEM-MILLED GAGE CHANGE AT LOCATION

Figure 8. Specimen 1 Sheet Thickness Before And After Chem-Milling

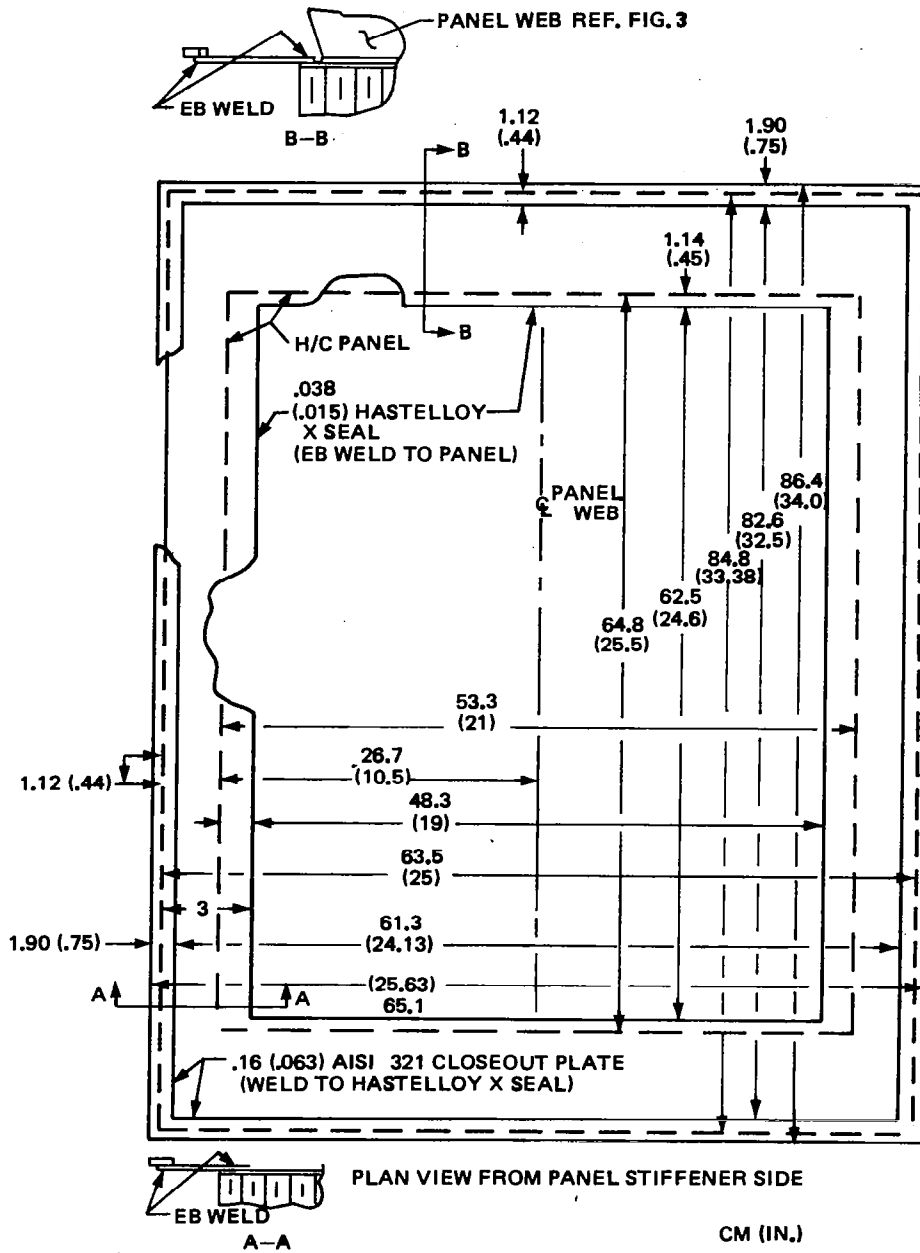


Figure 9. Specimen 1 Seal To Test Fixture

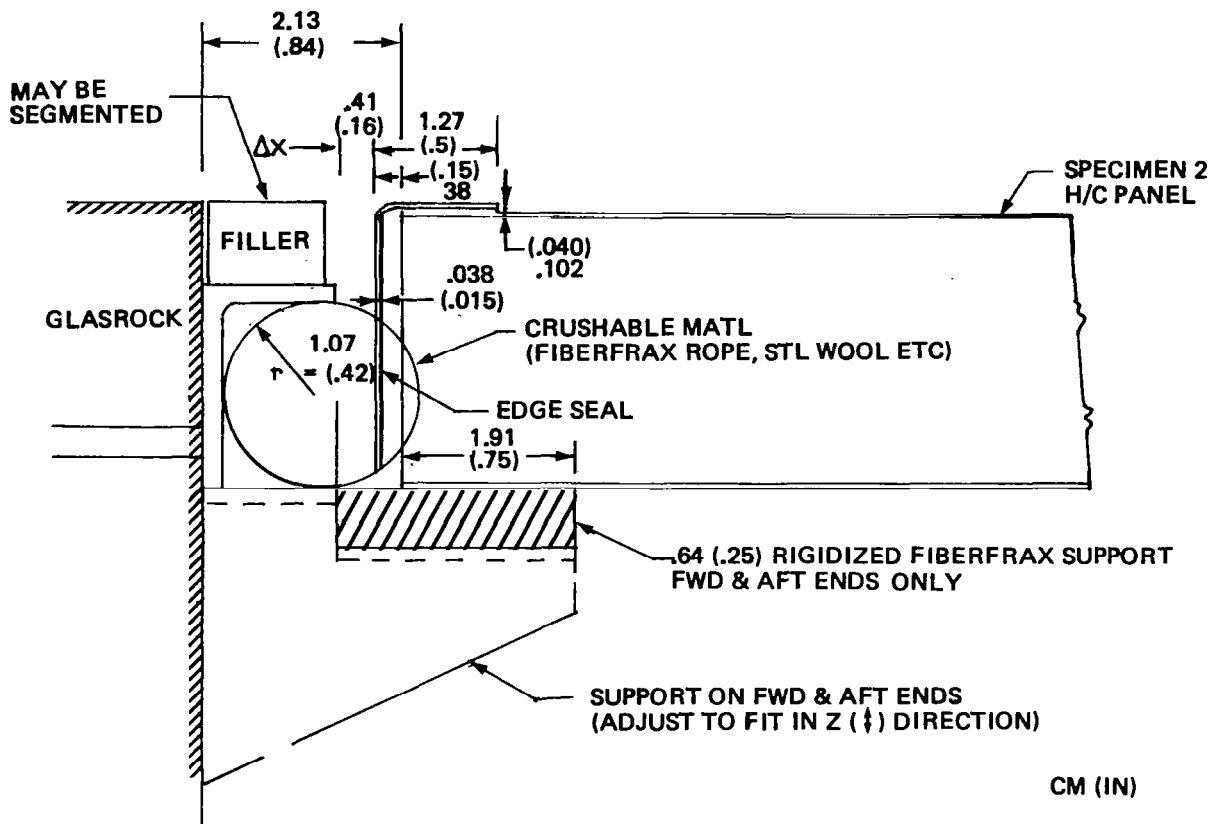


Figure 10. Specimen 2 NASA LaRC High Temperature Structures Wind Tunnel Interface Forward And Aft Edges

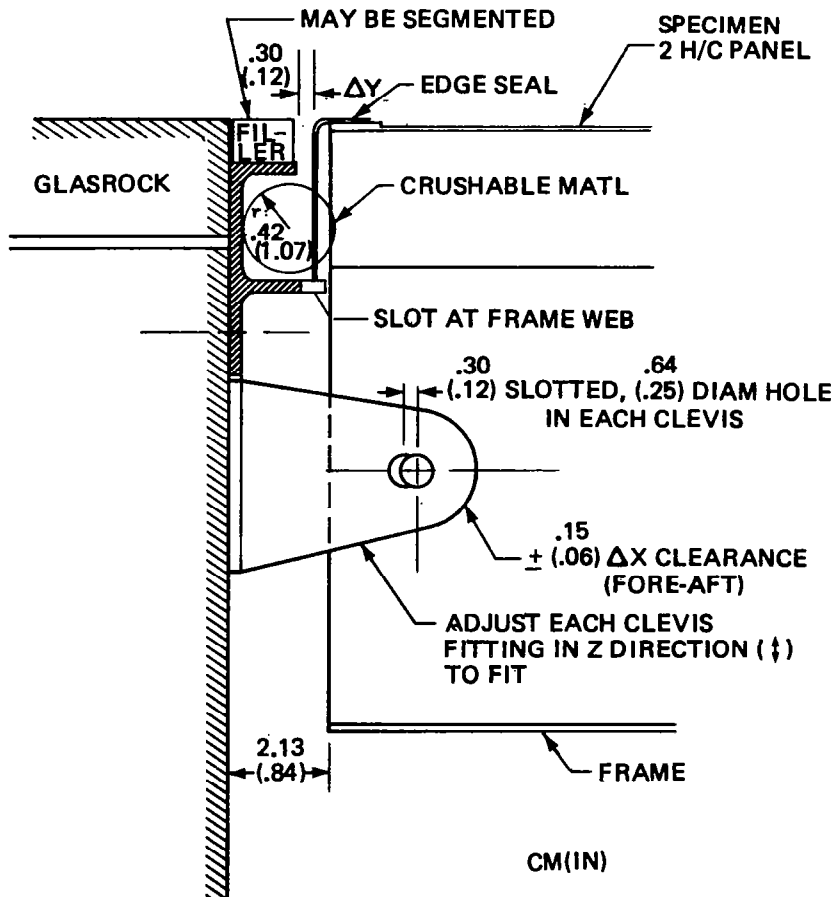


Figure 11. Specimen 2 NASA LaRC High Temperature Structures Interface~Long Side Edges

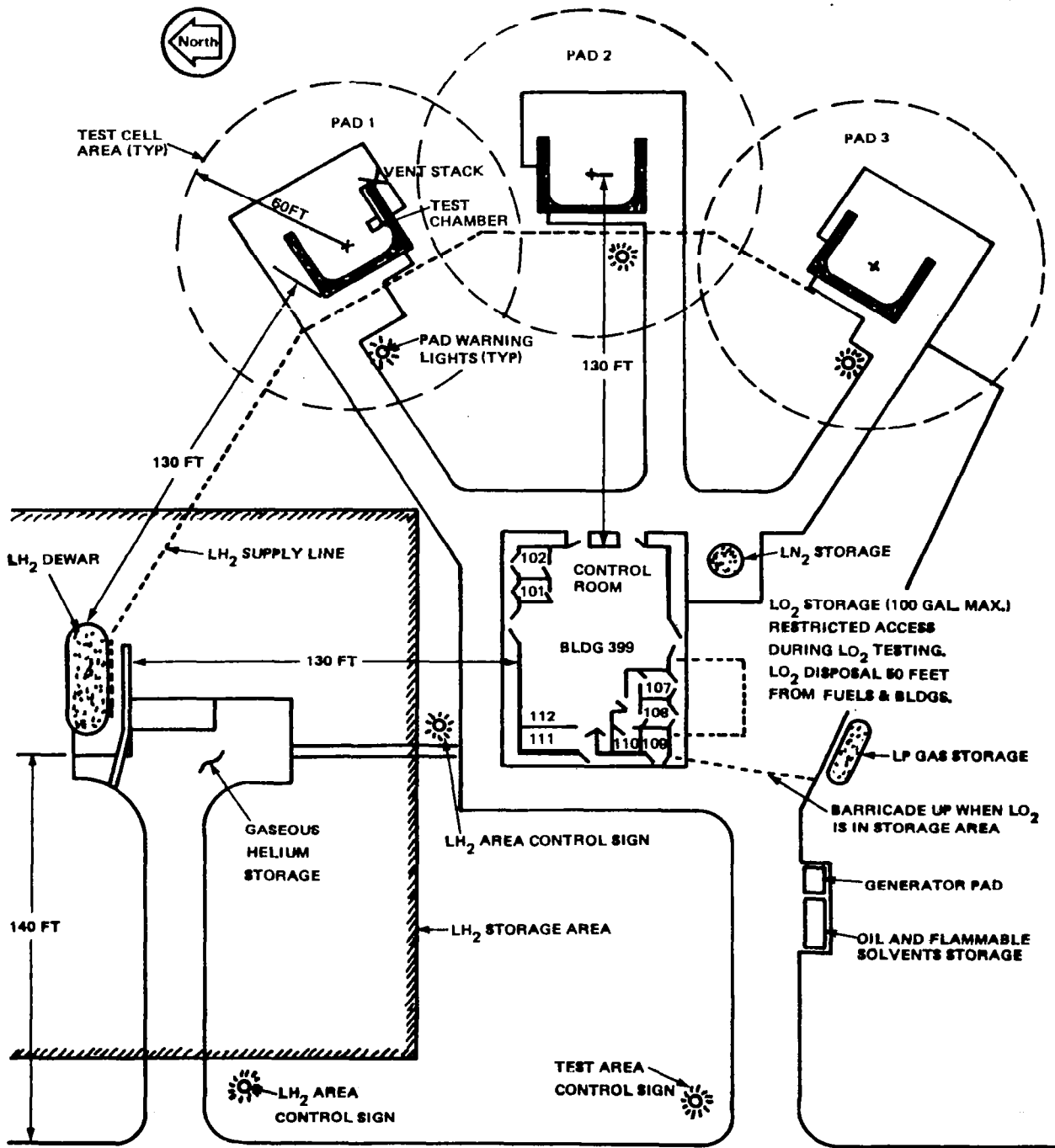


Figure 12. Test Area 41 Tulalip Test Site

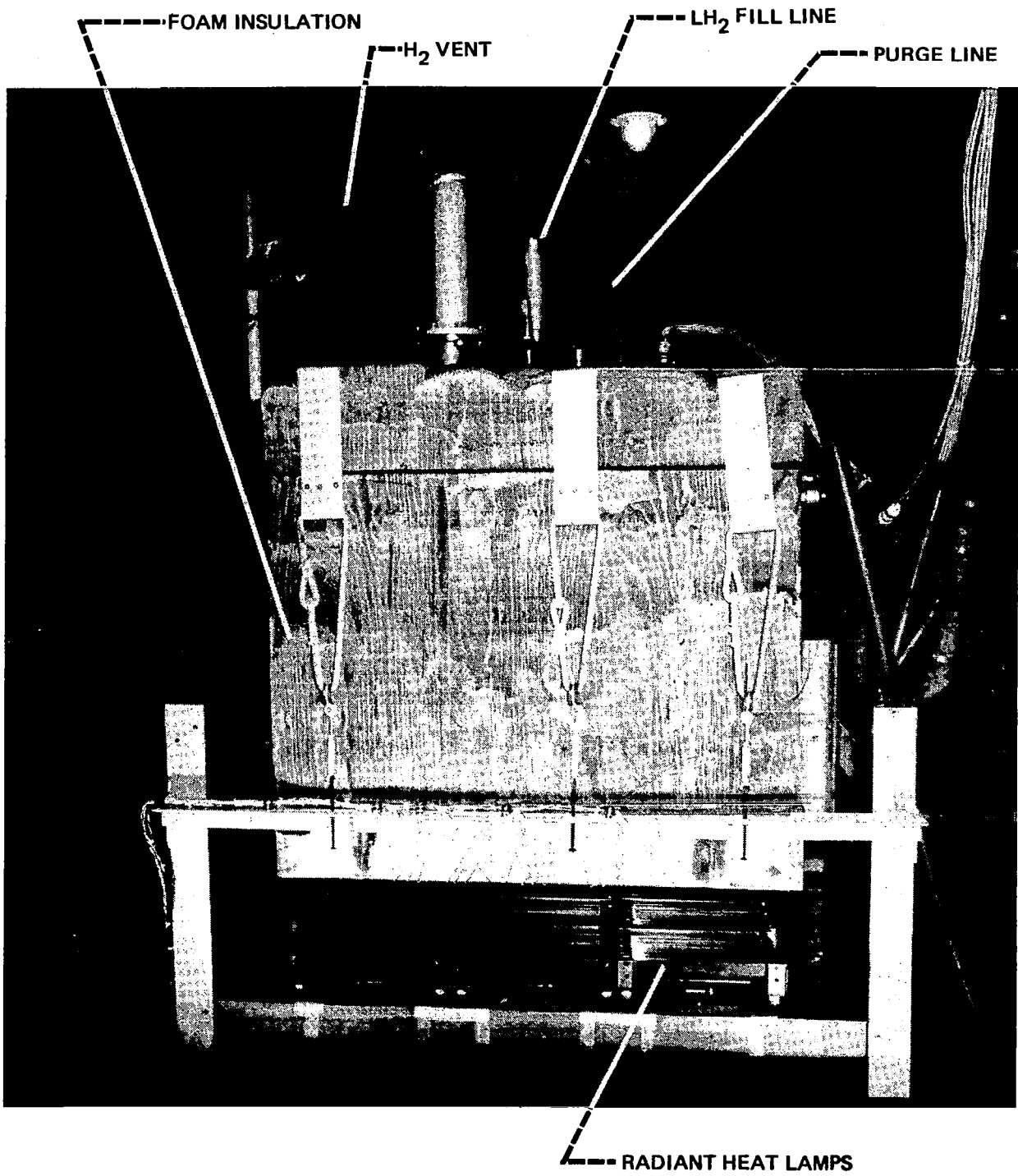


Figure 13. Specimen 1 Liquid Hydrogen and Radiant Heat Lamp Test Setup

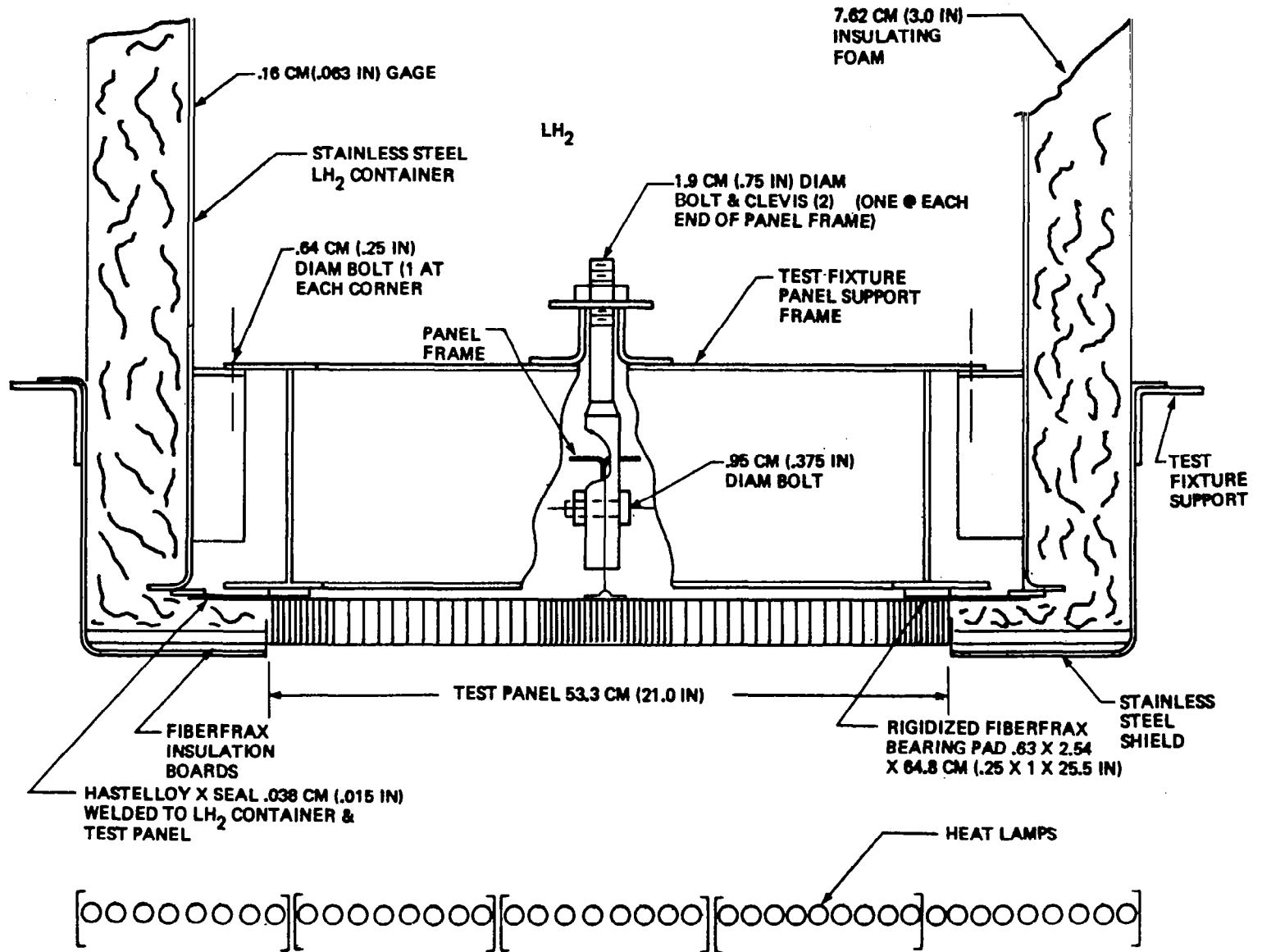


Figure 14. Specimen 1 Test Fixture Mounting

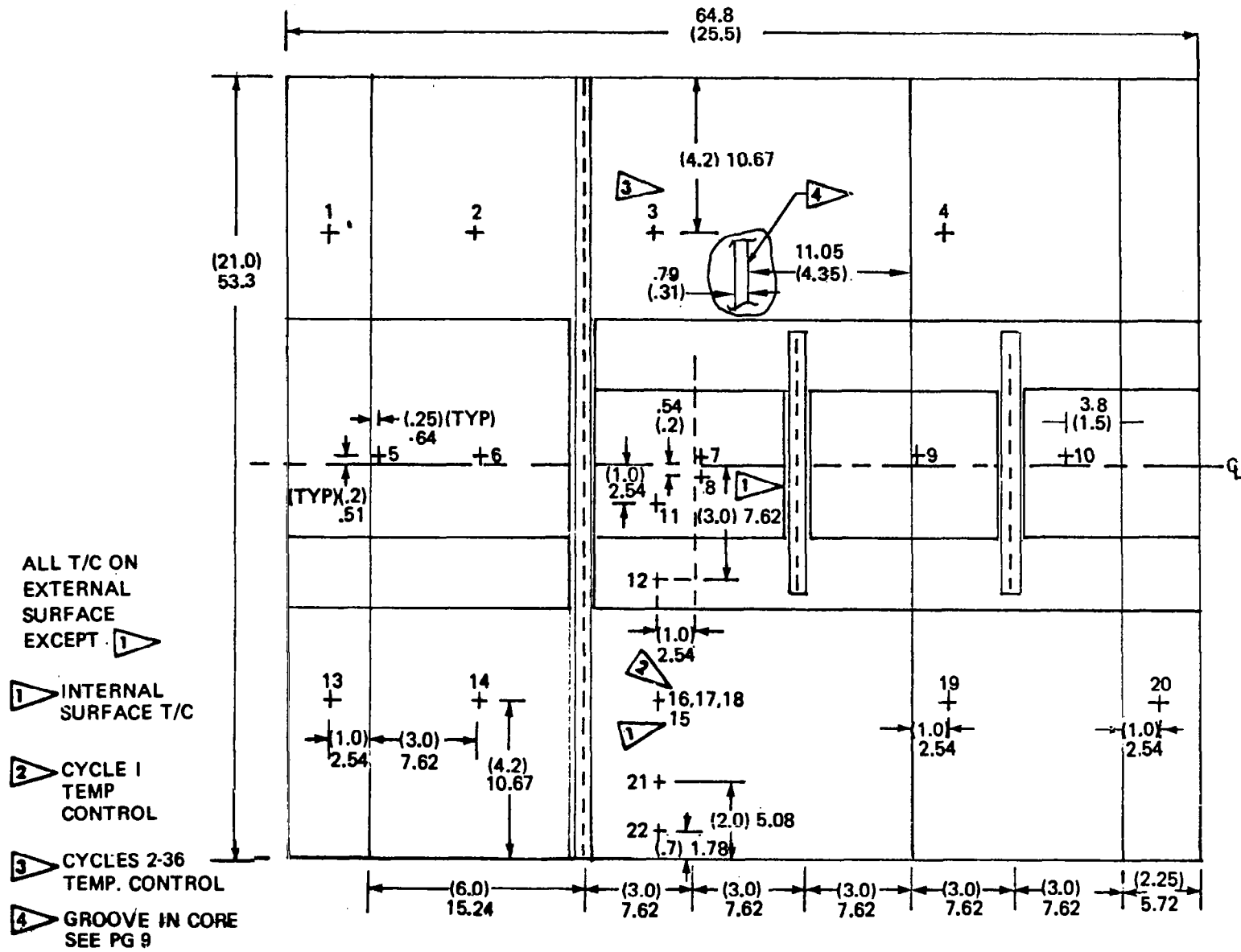


Figure 15. Specimen 1 Thermocouple Layout

ACTION	ACCUMULATED CYCLES	TIME (MIN.)	LH ₂ FLOW (GAL)*	LH ₂ FLOWRATE (GAL/MIN)*
Cool Down		90	369	(1.7 + 2.4)
Stabilize	9	20 10 180 60 20	48 24 720 144 80	2.4 2.4 4.0 2.4 4.0
Temp				
Hold				
9 Cycles				
Hold				
1 Cycle	10	290	1016	
Purge		90		
Inspect		480 (8 Hours)		
Cooldown		90	369	(1.7 + 2.4)
20 Cycles	30	582	2032	
		1.1 Days	3786	
Purge		90		
Inspect		480		
Cooldown		90	369	(1.7 + 2.4)
20 Cycles	50	582	2032	
		2.0 Days	6187	
Purge		90		
Inspect		480		
Cooldown		90	369	(1.7 + 2.4)
50 Cycles	100	1452	5080	
			11636	
Purge		90		
		3.5 Days		

* These rates are based on heat exchange and loss rates. Since half the LH₂ vaporizes during transfer to Pad 1 the computed LH₂ requirements at Pad 1 were multiplied by two (2) to determine LH₂ flow out of the dewar.

1 ▷ LH₂ only.

2 ▷ Thermal (Radiant Heat Lamp) Exposure Figure 7

3 ▷ Testing in groups of ten cycles - follows procedure of first 10 cycles including holding 1 hour with LH₂ exposure every 10 cycles after the ninth cycle.

Figure 16. Specimen 1 Test Plan Summary

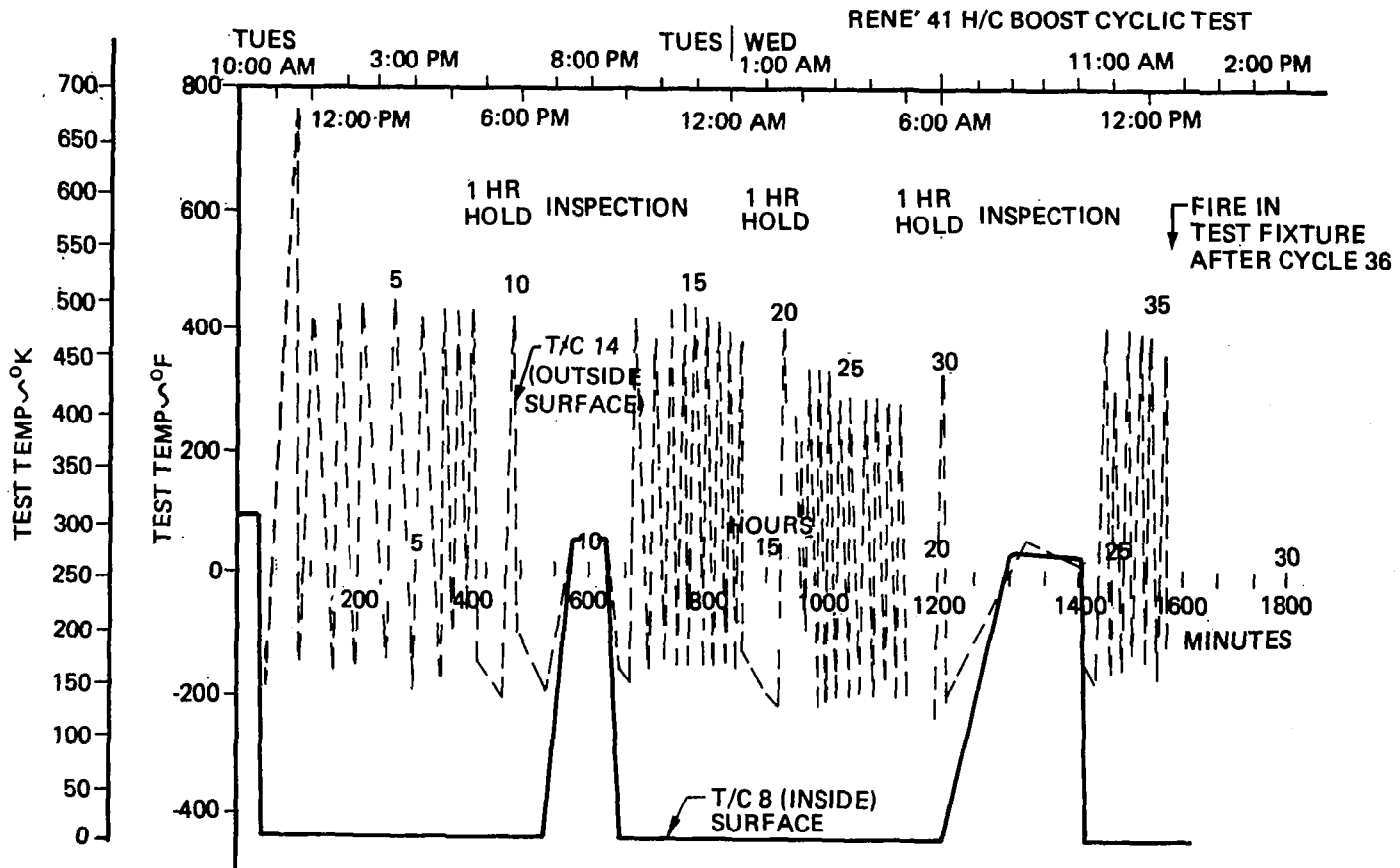


Figure 17. Specimen 1 Maximum & Minimum Inside And Outside Surface Temperatures

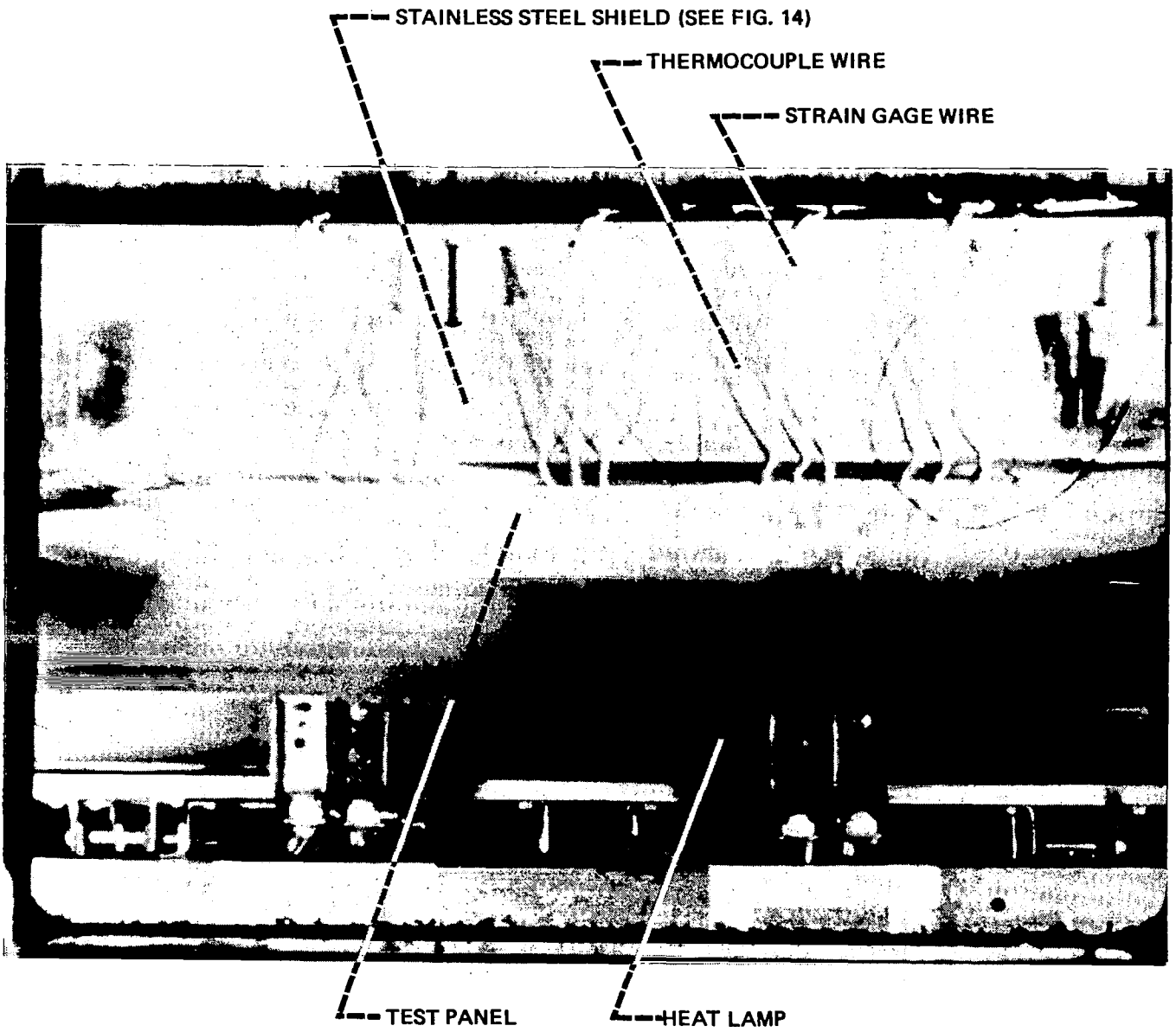


Figure 18. Specimen 1 Frost Formation Forty Minutes after Cool Down Following the Tenth Cycle

T/C	TEST CHANNEL	TIME	TEMPERATURE - K																					
		HOUR	*																					
		MINUTE	26	27	28	29	29	30	30	31	31	32	32	33	33	34	34	35	36	37	38	40	44	46
SECOND	20	20	50	20	50	20	50	20	50	20	50	20	50	20	50	20	50	20	20	20	20	20	20	
1	1		236	252	293	345	388	421	453	468	511	539	517	488	466	444	426	408	372	336	304	182	151	148
2	2		211	229	321	380	443	498	556	572	624	651	585	512	461	380	341	314	289	244	226	203	186	180
3	3		192	217	326	391	460	522	570	586	632	682	589	494	426	374	334	301	257	237	222	201	181	179
4	4		255	277	319	350	381	411	449	460	494	522	492	465	446	426	413	391	355	294	275	253	216	202
5	5		81	84	92	106	112	118	118	117	124	140	135	121	96	99	95	88	83	84	82	81	81	81
6	6		181	182	203	217	294	334	385	429	483	530	504	452	255	216	8	81	81	216	190	203	210	206
7	7		181	187	202	205	207	198	201	215	211	237	222	227	230	222	237	234	241	231	225	220	205	193
8	8		20	20	20	20	20	20	20	20	20	20	20	20	20	20	20	20	20	20	20	20	20	20
9	9		168	172	197	202	219	211	251	300	367	443	399	353	339	317	307	297	172	109	76	98	83	81
10	15		210	209	262	291	359	377	410	446	502	530	506	470	396	353	172	75	74	74	74	73	136	125
11	11		286	295	321	340	365	388	420	433	463	418	420	413	399	393	380	364	356	349	337	310	302	301
12	12		247	260	301	321	347	370	410	424	451	475	456	440	421	403	386	377	353	333	259	229	212	210
13	13		130	163	270	317	358	481	562	570	557	630	569	479	416	369	336	300	257	230	210	183	162	155
14	14		152	182	313	388	477	539	609	605	665	679	578	483	418	368	329	299	259	235	218	198	181	177
19	18		238	250	304	336	376	452	537	521	524	514	471	445	425	408	394	381	358	337	321	299	270	258
20	19		220	232	289	320	358	373	403	409	440	455	422	402	385	369	358	346	330	318	309	293	269	257
21	21		218	237	306	339	378	405	448	464	515	544	507	477	451	359	280	222	183	192	186	147	145	160
22	22		184	192	257	301	337	346	394	424	474	460	421	354	307	280	274	262	261	246	245	236	224	205

Ref. Figure 15 for T/C locations

▷ 10:36.20 October 14, 1980 T/C 8 First Registered Change from Ambient Temp.

* Maximum Temperature

Figure 19. Specimen 1 First Cycle Heat Pulse

T/C	TEST CHANNEL	TIME	TEMPERATURE - °F																					
		HOUR	*																					
		MINUTE	26	27	28	29	29	30	30	31	31	32	32	33	33	34	34	35	36	37	38	40	44	46
SECOND	20	20	50	20	50	20	50	20	50	20	50	20	50	20	50	20	50	20	50	20	20	20	20	
1	1		-34	-6	68	161	238	299	356	382	460	510	471	419	380	340	307	275	210	145	88	-132	-188	-192
2	2		-80	-48	118	224	337	437	541	569	664	711	593	462	370	225	154	106	61	-20	-53	-93	-125	-135
3	3		-114	-68	127	244	368	480	566	595	678	768	601	430	307	213	141	83	4	-32	-60	-98	-133	-137
4	4		0	40	114	171	227	281	348	369	430	479	426	377	344	307	283	244	179	69	36	-4	-71	-95
5	5		-314	-308	-293	-268	-258	-247	-247	-248	-236	-207	-216	-242	-287	-281	-289	-300	-309	-308	-311	-314	-314	-314
6	6		-133	-132	-93	-68	69	141	233	313	409	495	448	354	0	-70	-313	-313	-314	-70	-117	-94	-81	-88
7	7		-134	-123	-95	-90	-86	-102	-97	-73	-79	-33	-59	-50	-45	-60	-33	-38	-25	-43	-54	-64	-91	-111
8	8		-423	-423	-423	-423	-423	-423	-423	-423	-423	-423	-423	-423	-423	-423	-423	-423	-423	-423	-423	-423	-423	-423
9	9		-157	-150	-104	-96	-66	-79	-7	80	201	337	258	175	150	111	93	76	-150	-263	-323	-283	-310	-313
10	15		-82	-83	12	64	186	219	278	343	443	494	451	386	253	176	-150	-324	-326	-326	-326	-327	-215	-234
11	11		56	71	118	153	197	238	297	320	374	293	296	284	259	247	225	196	182	169	148	98	84	83
12	12		-14	9	83	119	166	206	279	304	352	395	361	332	299	266	236	219	176	140	6	-47	-78	-81
13	13		-226	-166	26	112	184	407	552	566	542	674	564	402	289	204	145	80	3	-45	-82	-130	-167	-180
14	14		-186	-132	104	238	399	511	636	630	737	762	580	410	292	203	133	79	6	-37	-67	-102	-134	-140
19	18		-31	-9	88	145	217	354	507	478	484	466	388	341	305	274	250	227	184	147	118	79	27	5
20	19		-63	-42	61	116	184	211	265	276	332	359	300	264	233	204	184	163	134	113	96	68	24	3
21	21		-67	-32	91	150	220	270	346	376	467	520	452	399	352	187	45	-60	-129	-113	-124	-195	-199	-172
22	22		-128	-113	4	83	147	164	250	303	394	369	298	177	93	45	34	12	10	-16	-19	-35	-57	-90

Ref. Figure 15 for T/C locations

▷ 10:36.20 October 14, 1980 T/C 8 First Registered Change From Ambient Temp.

* Max. Temperature

Figure 20. Specimen 1 First Cycle Heat Pulse

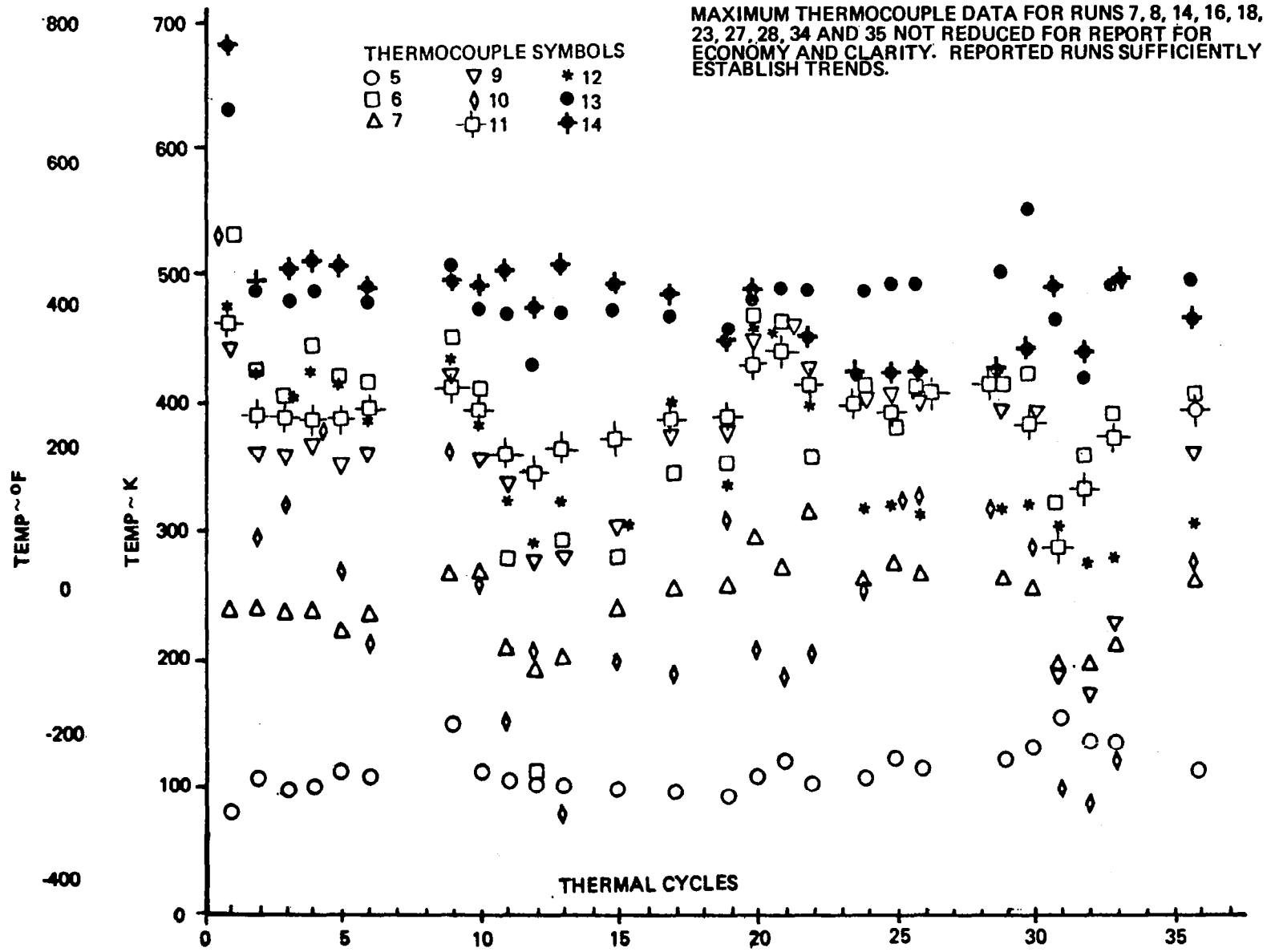


Figure 21. Maximum Thermocouple Readings During Cyclic Exposure. See Figure 15 for Thermocouple Locations

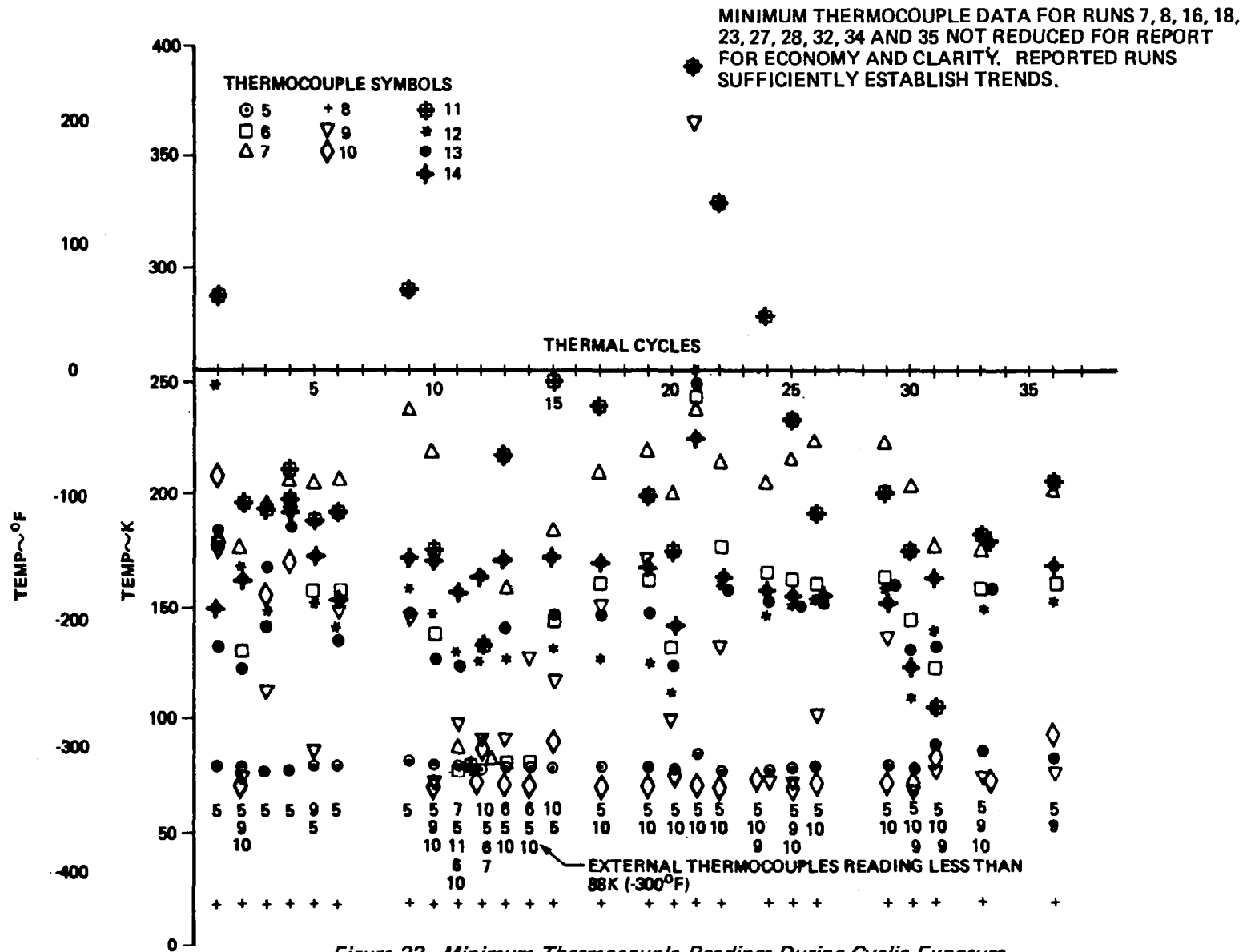


Figure 22. Minimum Thermocouple Readings During Cyclic Exposure
See Figure 15 for Thermocouple Locations

APPENDIX A
PANEL DESIGN ANALYSIS

TABLE OF CONTENTS

Appendix A

	<u>PAGE</u>
PANEL DESIGN ANALYSIS	53
Design Data	54
Finite Element Model	54
Core Stresses	55
SKIN STRESSES	58

LIST OF FIGURES

Appendix A

<u>NO.</u>	<u>TITLE</u>	<u>PAGE</u>
A-1	Specimen 1 Shear & Moment Diagrams for Boost Thermal Environment . .	60
A-2	Specimen 2 Shear and Moment Diagrams for Entry Thermal Environment .	61
A-3	Approximate Relationships Between Ref. 3 Vehicle and Specimen 1 Moment and Average Shear Load	62
A-4	Specimen 1 Finite Element Model	63
A-5	Specimen 1 Finite Element Model Outer Skin Input Data	64
A-6	Specimen 1 Finite Element Model Inner Skin Input Data	65
A-7	Specimen 1 Finite Element Model Honeycomb Core Properties	66
A-8	Specimen 1 Finite Element Model Frame & Core Z & Y Coordinates . . .	67
A-9	Specimen 1 FEM Longitudinal Core Shear Stresses	68
A-10	Specimen 1 Transverse Core Shear Stresses	69
A-11	Specimen 1 Core Normal Stresses at Frame Due to Thermal Loads . . .	70
A-12	Specimen 1 Outer Skin Inplane Stresses	71
A-13	Specimen 1 Outer Skin Inplane Stresses	72
A-14	Specimen 1 Inner Skin Inplane Stresses	73
A-15	Specimen 1 Inner Skin Inplane Stresses	74
A-16	Specimen 2 HTST Test Average Skin Stresses See Figure A-2 for Load Condition	75

Appendix A

PANEL DESIGN ANALYSIS

This appendix contains a structural analysis of the Rene'41 honeycomb test panel and shows the effect of the slotted face sheet on core and face sheet stresses.

Longitudinal shear and moment diagrams of Specimens 1 and 2 for the test conditions are shown in Figures A-1 and A-2, respectively. These diagrams show only the overall test panel reaction to the heating environment. Figure A-3 shows a schematic comparison of Specimen 1 moments and average shear loads to those of the Ref. 3 vehicle panel. In the typical wing and body surface panel of the Ref. 3 vehicle, the average thermal environment produces a constant moment. Thus, the thermal environment produces zero average shear load in panels spanning a large number of equally spaced frames. The Ref. 3 vehicle boost loads also include fuel pressure induced loads. Specimen 1 is sized so that the test shears produced fall within the range of shear loads induced by Ref. 3 vehicle fuel pressure loads.

Although, the Ref. 3 vehicle is primarily designed and sized by boost loads, entry temperatures are paramount in materials selection. Vehicle loads are much lower at maximum external surface temperature during entry because tankage pressures are low after fuel exhaustion at the end of the boost phase and internal and external surface panel temperatures are nearly equal. Specimen 2 does pick up some thermally induced shear loads as shown in Figure A-2 that are not present in the Ref. 3 vehicle.

Design Data

The panel design and analysis was based on the following limit and ultimate stress levels. Design limit tension stress for Rene'41 structure was taken to be 689 MPa (100 ksi) at 20K (-423⁰F). Design limit compression stress was taken to be 607 MPa (88 ksi) at 478K (400⁰F). Design ultimate compression stress was taken to be 758 MPa (110 ksi) and .0058 strain at 478K (400⁰F). Typical room temperature longitudinal core shear failure stress determined from limited test data is 0.93 MPa (135 psi) for the 75.3 kg/m³ (4.7 lb/ft³) core and is 3.37 MPa (490 psi) for the 150.6 kg/m³ (9.4 lb/ft³) core. The estimated longitudinal shear failure stress for 221.1 kg/m³ (13.8 lb/ft³) and for 301.2 kg/m³ (18.8 lb/ft³) core are approximately 7.38 MPa (1070 psi) and 13.6 MPa (1970 psi) respectively. The core crushing stress of the 301.2 kg/m³ (18.8 lb/ft³) core is approximately 29 MPa (4200 psi) at room temperature.

Finite Element Model

A finite element analysis was developed to determine the internal loads of Specimen 1. The overall finite element model (FEM) used in this analysis is displayed in Figure A-4. The temperatures used to determine the thermal expansion inputs to the finite element model, its skin gages and elastic modulus are displayed in Figure A-5 for the outer skin and Figure A-6 for the inner skin. The FEM core densities and elastic properties are shown in Figure A-7. The FEM nodal coordinates are displayed in Figures A-7 and A-8. Minor skin gage variations which exist between the FEM and the Specimen 1 drawing (Figures 1, 2 and 3 are shown in Figures A-5 and A-6. These variations are a result of minor changes made after the FEM analysis, but which did not warrant re-analysis.

Core Stresses

Longitudinal core shear stresses for Specimen 1 generated by the finite element analysis are plotted in Figure A-9. As previously mentioned, test specimen reaction induced core shear stresses are not found as thermally induced stresses on the Ref. 3 vehicle but are approximately equivalent to the Ref. 3 vehicle fuel pressure induced shear stress. The average longitudinal core shear stress was approximately 1.59 MPa (230 psi). This value was approximately 1.45 MPa (210 psi) for the test specimen design. These values differ because of skin gage differences between the design and the FEM.

The shapes of the longitudinal core shear stress curves shown in Figure A-9 are characteristic of the core shear stresses found in the Ref. 3 vehicle adjacent to frames. The stresses are caused by the frame's resistance to panel thermal deformation in the Z direction. The short 15.2 cm (6 in.) intermediate slot located midway between the continuous slots on 15.2 cm (6 in.) spacing has a small additional influence on this panel thermal deformation or bowing and hence causes an additional reduction of longitudinal and transverse shear stress as shown in Figures A-9 and A-10. These reductions may be seen on Figures A-9 and A-10 by comparing stresses at $Y = 0$ to those at $Y = 15.2$ cm (6 in.) which are influenced by the short intermediate slot.

The Specimen 1 finite element model transverse core shear stresses at and near the frame are plotted in Figure A-10. These stresses are a close approximation of the Ref. 3 vehicle transverse core shear stresses. The transverse core shear stresses are caused by the contraction of the inner skin and frame under cryogenic temperatures and the expansion of the outer skin at boost temperatures while the panel is being held relatively flat by the stiff frame. The transverse core shear stresses are lowered drastically at small distances away from the frame because the panel is more free to deform or bow in the

Z direction away from the frame. As previously mentioned, the transverse core shear is generally reduced by locating a short slot midway between the continuous slots. The higher value at $Y = 30.5$ cm (12 in.) may be influenced by its proximity to the Z reaction point at $Y = 29.2$ cm (11.5 in.).

Specimen 1 FEM developed panel normal loads at the frame were used to calculate the core normal stresses plotted in Figure A-11. These thermally induced normal loads are similar to those present in the Ref. 3 vehicle except for an average stress of 3.24 MPa (470 psi) included in Figure A-11 which is caused by the test reaction loads (See Fig. A-1 for these reaction loads). These thermal loads (except for the reaction loads) are caused by the thermally deformed panel being forced to conform to the relatively stiff frame. The frame flange and locally heavy inner skin near the frame assist the core in carrying the shear load and help to distribute the normal loads required to form the panel in the Z direction at the frame. A width of 1.52 cm (0.6 in.) on either side of the frame was used in determining the core normal stresses as described in Figure A-11. The inner skin and frame flange configuration are shown in Figure 3.

The exact crushing strength of the Rene'41 RCB N2-20 core used at the frame as shown in Figure 3 is not yet known. The density of this core is 301 kg/m^3 (18.8 lb/ft^3). As mentioned previously, its core crushing strength is estimated at 29 MPa (4200 psi) at room temperature. The core compression load is introduced by shear causing the average stress level to be one half the maximum stress. The small cell size of .32 cm (.125 in.) with the .005 cm (.002 in.) foil should make the core relatively stable. This core stability combined with load being introduced by shear should allow the core cell wall to achieve compression yield stress at the inner skin. Temperatures in the core at the frame range from 20K (-423°F) on the inner skin to 425K (305°F) on the outer

skin. The compression yield stress in the core material near the inner skin will be approximately 1018 MPa (148 ksi) at a temperature of 122K (-240⁰F). The core ultimate compression stress will be approximately 37 MPa (5370 psi) based on core area if the core is fully stable with its compression load being introduced by shear. On Figure A-11 it is noted that the core stress varies from -23 MPa (-3300 psi) to -2 MPa (-300 psi) within 1.27 cm (0.5 in.). Very small displacements in the Z direction under normal loads probably will cause a redistribution of this peak stress.

Specimen 1 provides an interesting demonstration of the combination of high longitudinal, transverse and normal stresses in the honeycomb core at the frame and adjacent to the slots in the outer skin. The slots that reduce skin stresses, cause a local increase of core stresses at the frame. Proper spacing of the slots is necessary to make both skin stresses and core stresses manageable.

The stresses for Specimen 2 are expected to be low and are not shown in the Figures. The average longitudinal core shear stress for Specimen 2 from the end support to the frame is only 28 psi during the test. Peak transverse and longitudinal shears were not determined on Specimen 2. Specimen 2 differential temperatures between inner and outer skins will be 111K (200⁰F) as compared to 448K (800⁰F) on Specimen 1. As for Specimen 1, Specimen 2 also will experience longitudinal core shear stresses caused by the thermal environment that do not occur on the Reference 3 vehicle. These test-only longitudinal shear stresses result from the requirement to support the panel at its forward and aft edges to present a surface flush to the edge of the test fixture during the HTST hypersonic flow regime.

SKIN STRESSES

Specimen 1 FEM developed outer skin stresses which result from the boost thermal environment (See Figs. A-5 and A-6) are displayed in Figures A-12 and A-13, and inner skin stresses are shown in Figures A-14 and A-15. The purpose of the outer skin slots is to reduce longitudinal (X direction) thermal stress levels in the Ref. 3 vehicle by approximately 30% by allowing relatively free growth of the outer skin in the transverse (Y direction) during thermal expansion during boost and entry heating regimes. The slots cause the Ref. 3 transverse panel thermal stresses to be reduced to negligible values away from the frames. A very significant advantage in slotting the outer surface is in the fact that it eliminates the differential temperature between frame or spar and the outer skin from becoming a factor in generating high transverse stresses in both the boost and entry environments. The panel thermal moment at the frame on Specimen 1 closely approximates the combination of pressure and thermal moments on the Ref. 3 vehicle as shown in Figure A-3. The Ref. 3 vehicle thermally induced longitudinal and transverse skin stresses over many evenly spaced frames will be approximately two-thirds of the values shown in Figures A-12 through A-15 because the two span configuration of the test panel results in approximately a 50% increase in thermal moment at the frame relative to the vehicle under the same thermal conditions. In establishing specimen skin gages, some local skin gages used on the FEM analysis were changed to accommodate the loads established by that analysis. The .064 cm (.025 in.) gage outer skin over the frame was changed to .071 cm (.028 in.) as shown in Figure A-5. Final chem-milling produced an actual gage over the frame of .074 cm (.029 in.) as shown in Figure 8. Specimen 1 overall stresses will be slightly altered from the FEM because of a change of moment as noted in Figure A-1 caused by differences of inner and outer skin average thicknesses between the FEM and

the test specimen nominal and actual gages. The test specimen local stresses are also altered from the FEM by the small changes of local skin gages shown in Figures A-5, A-6 and 8. It is estimated that the maximum Specimen 1 longitudinal stress at the frame between the 15.24 cm (6 in.) spaced slots is approximately 586 MPa (85,000 psi) and 648 MPa (94,000 psi) between the 7.62 cm (3 in.) slots for nominal gages at the design temperatures.

Figures A-12 through A-15 show that a local increase in gage results in a drop in longitudinal stress level. Figures A-12 through A-15 show that thermally induced transverse skin stress values adjacent to the frame are lowered by decreasing slot spacing.

The Specimen 2 average skin stresses are shown in Figure A-16. The allowable intracell buckling stress of .038 cm (.015 in.) sheet on .953 cm (.375 in.) cell size core at 1033K (1400^oF) is approximately 478 MPa (69,400 psi). Compared to this allowable stress, the skin stress levels are low, which is also typical of Ref. 3 vehicle thermal stresses at maximum external temperature. The vehicle differential skin temperatures are a modest 111K (200^oF) at maximum temperature.

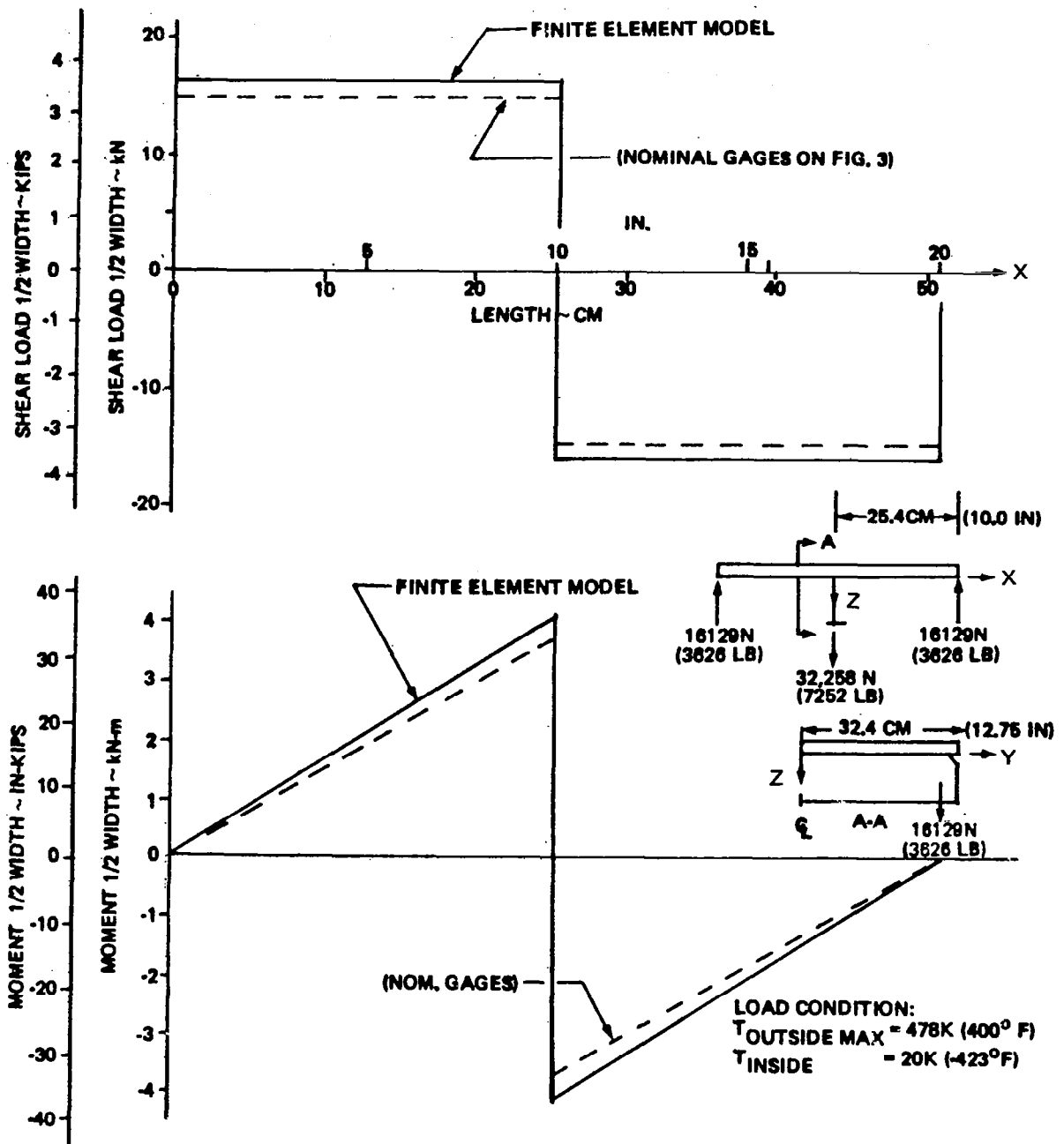


Figure A-1. Specimen 1 Shear & Moment Diagrams For Boost Thermal Environment

$T_{\text{OUTSIDE}} = 1034 \text{ K (1400}^\circ \text{ F)}$
 $T_{\text{INSIDE}} = 922 \text{ K (1200}^\circ \text{ F)}$

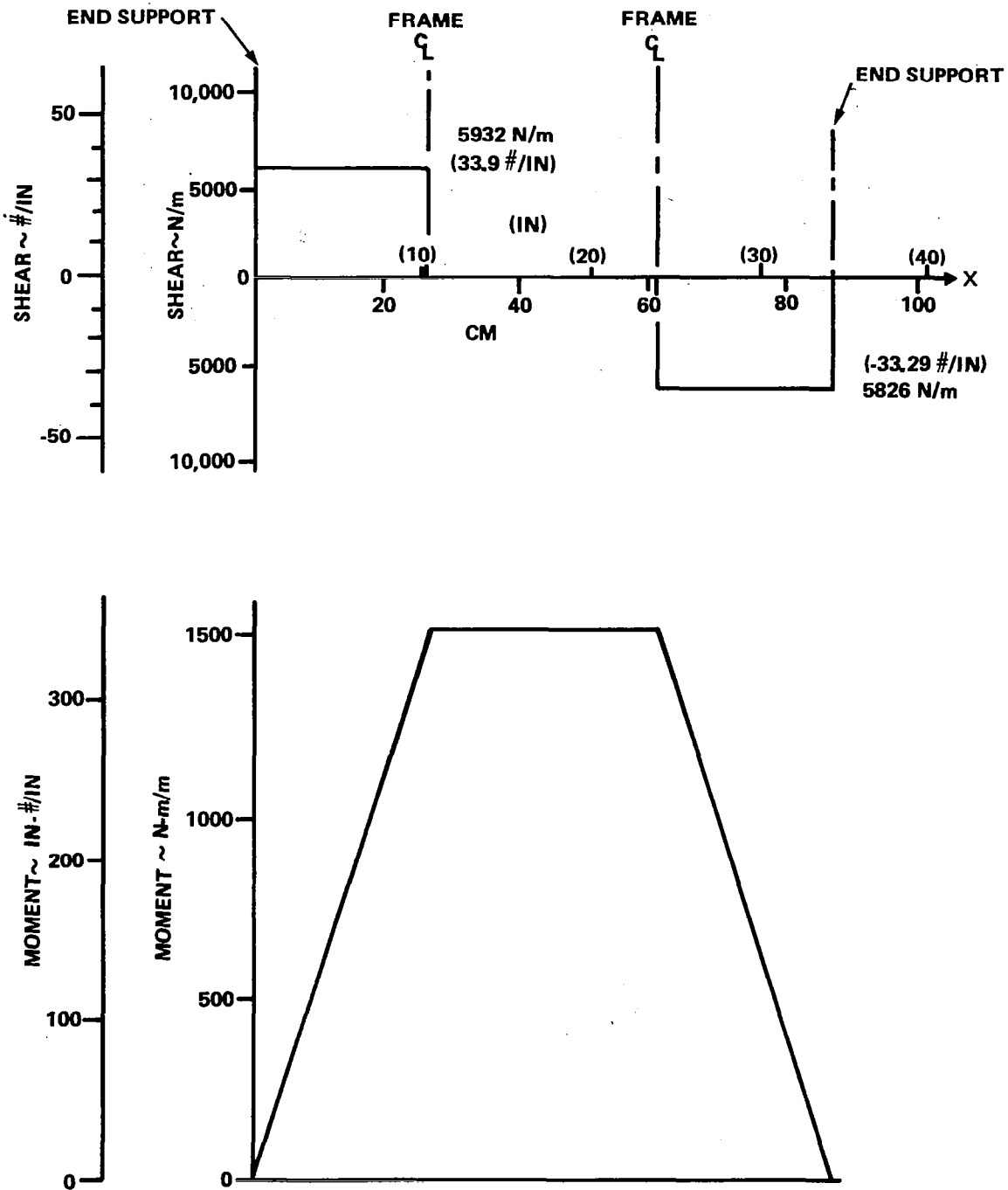


Figure A-2. Specimen 2 Shear And Moment Diagrams For Entry Thermal Environment

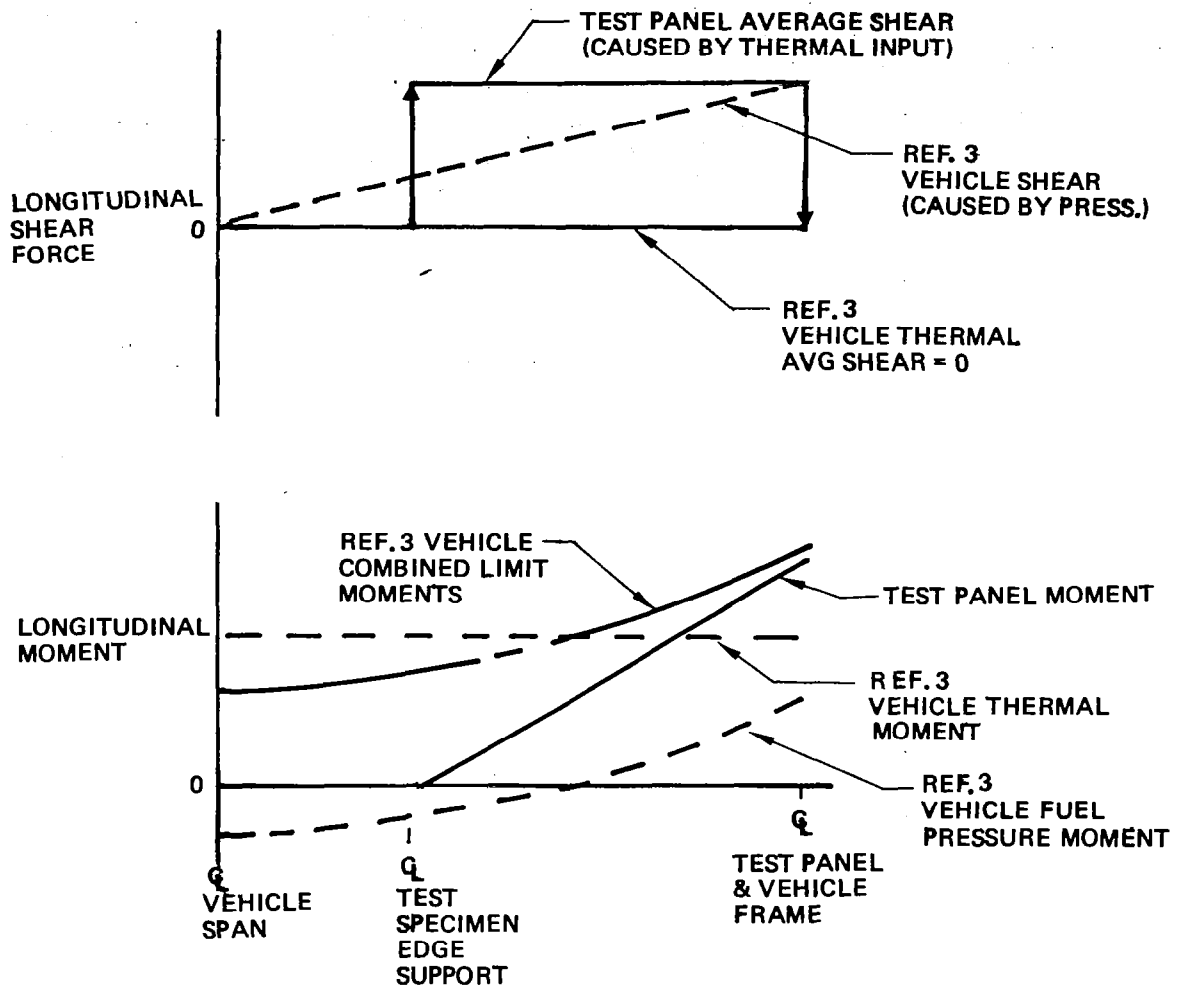


Figure A-3. Approximate Relationships Between Ref. 3 Vehicle and Specimen 1 Moment & Average Shear Load

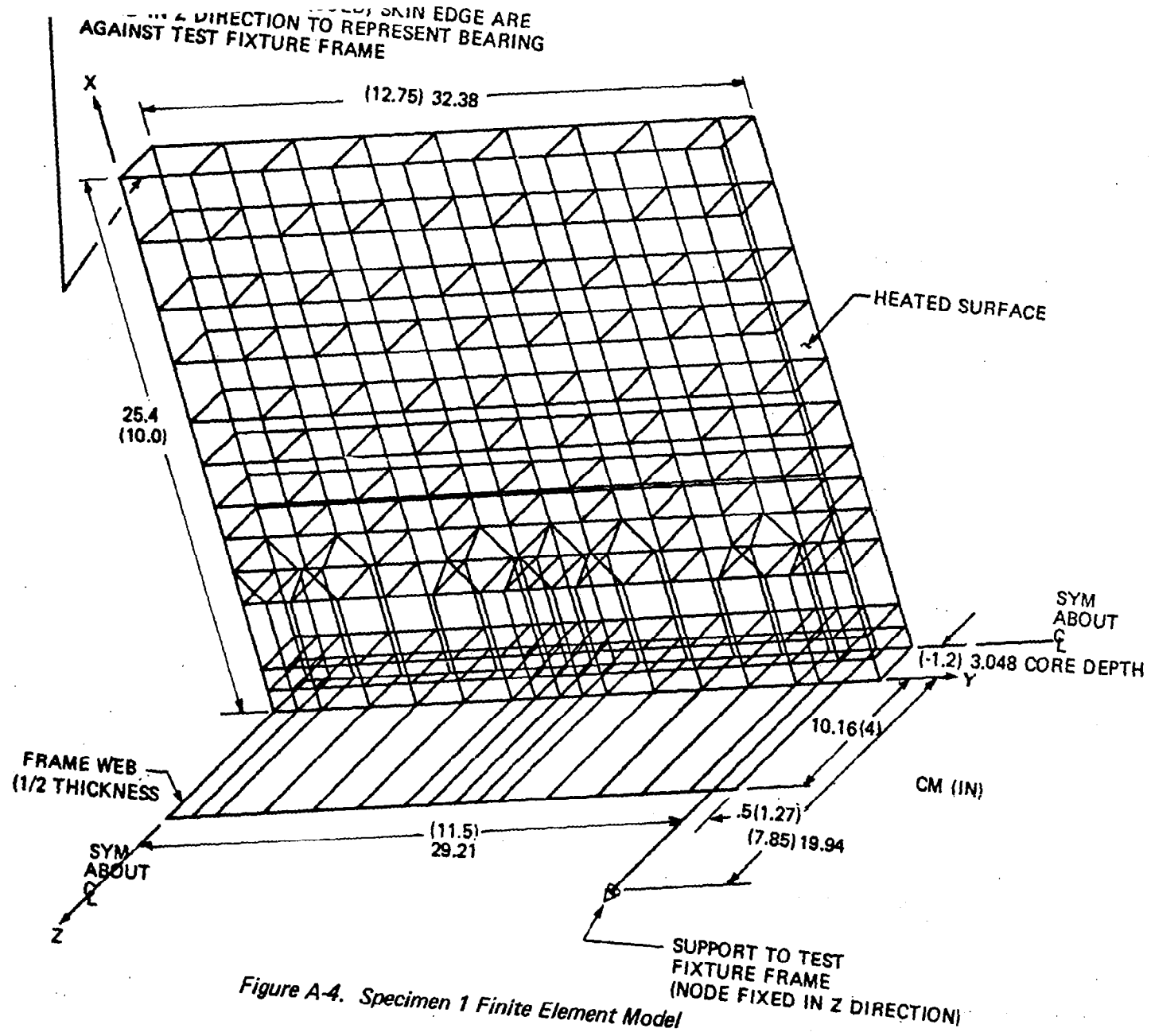


Figure A-4. Specimen 1 Finite Element Model

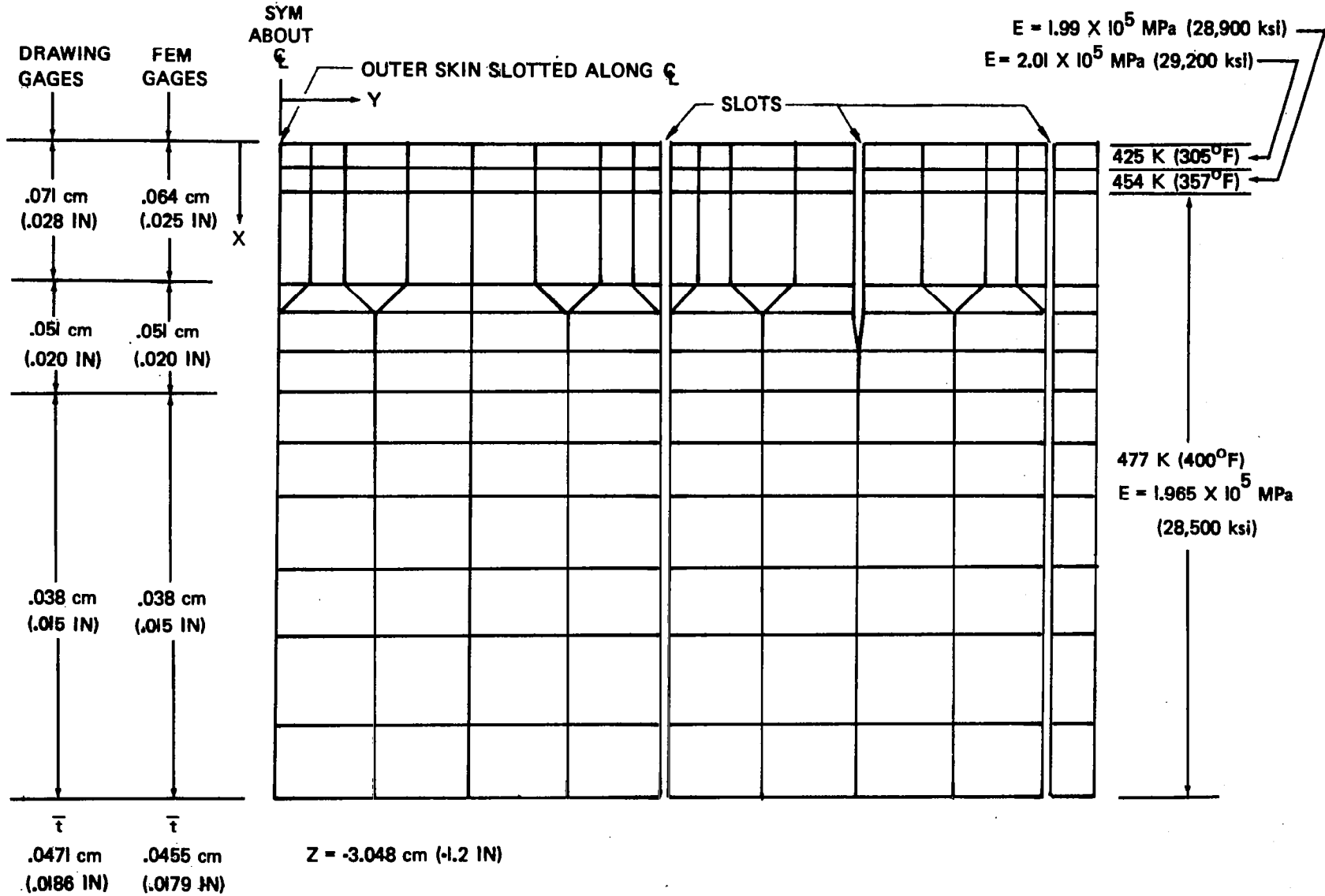


Figure A-5. Specimen 1 Finite Element Model Outer Skin Input Data

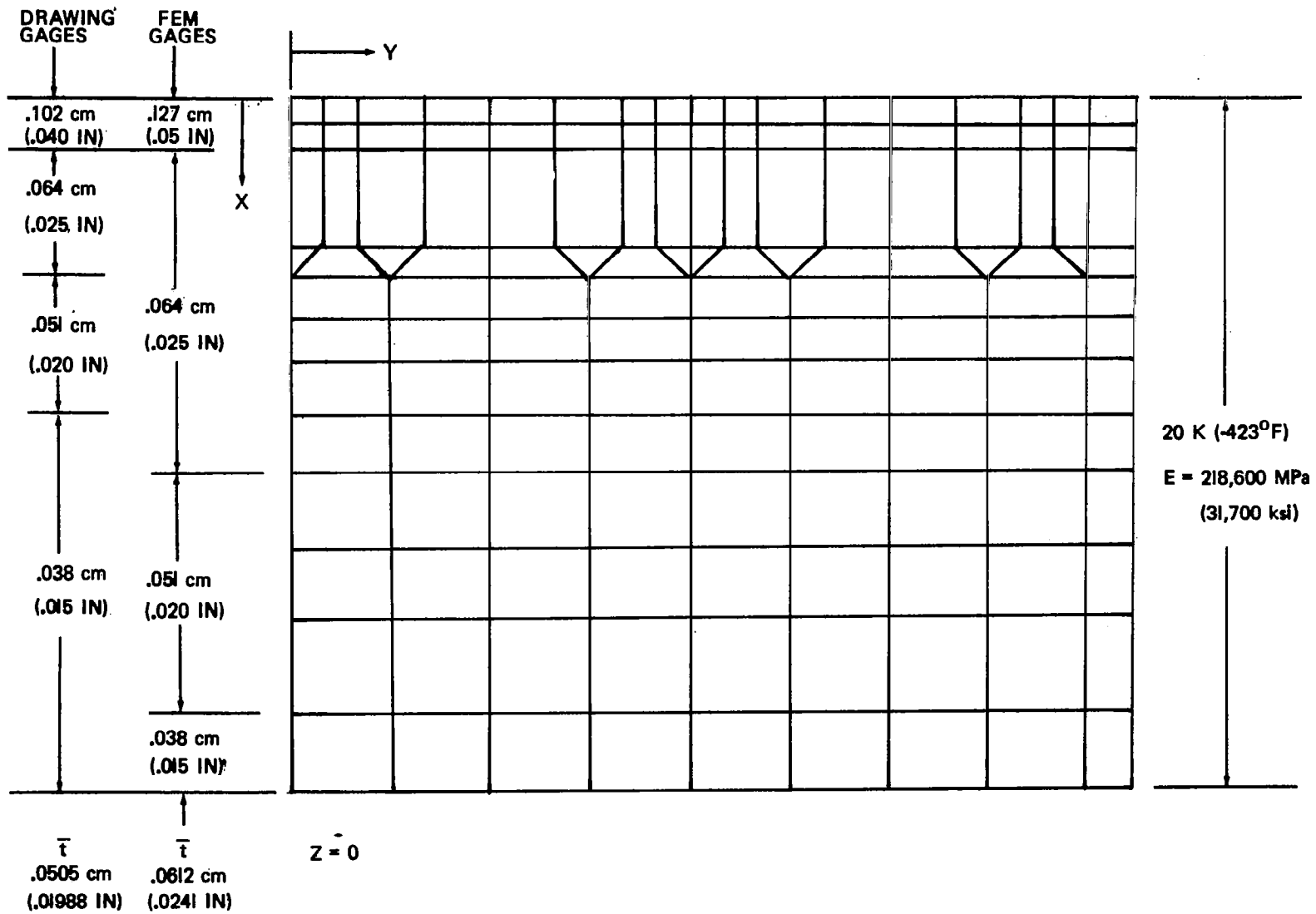


Figure A-6. Specimen 1 Finite Element Model Inner Skin Input Data

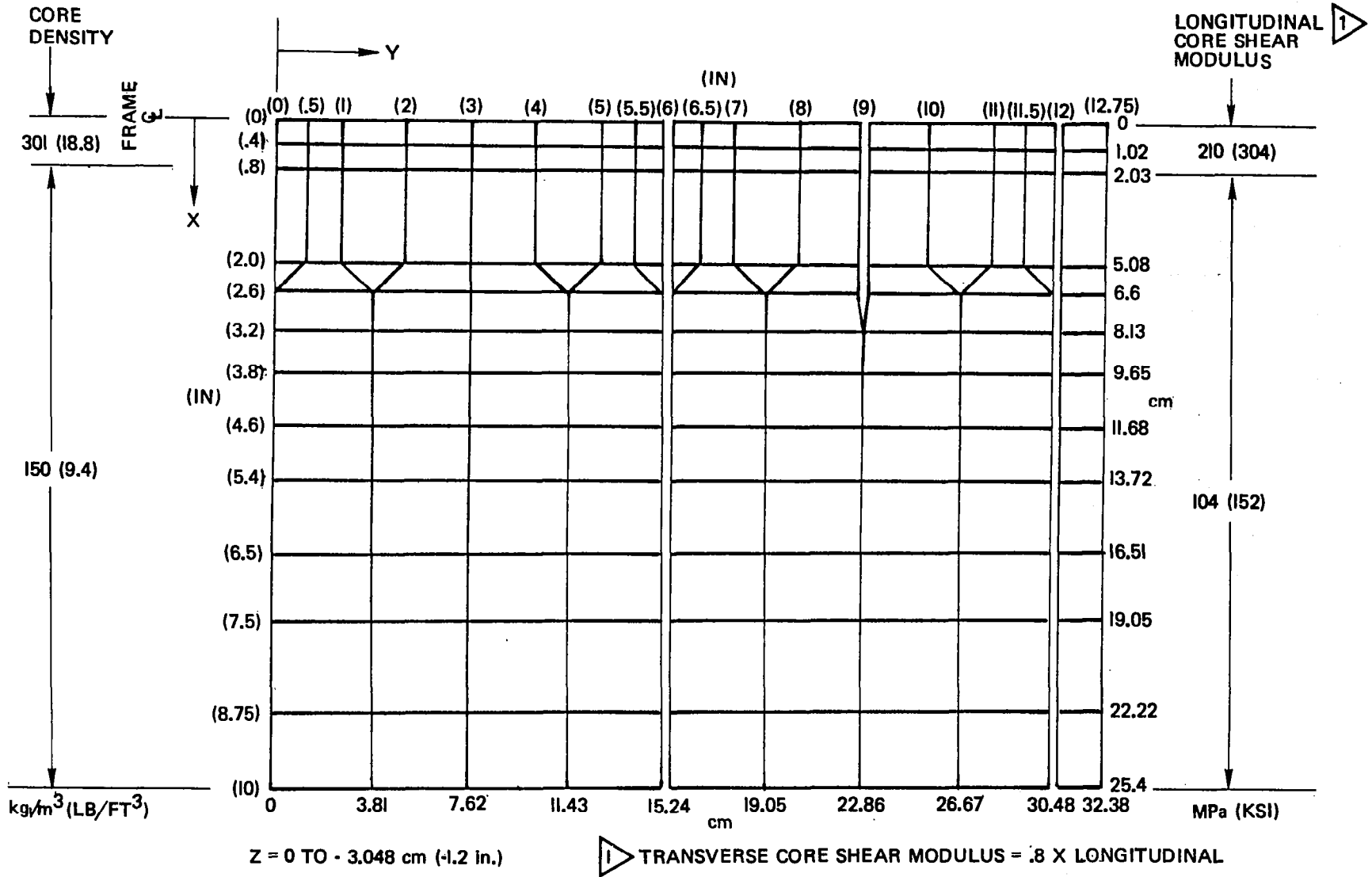


Figure A-7. Specimen 1 Finite Element Model Honeycomb Core Properties

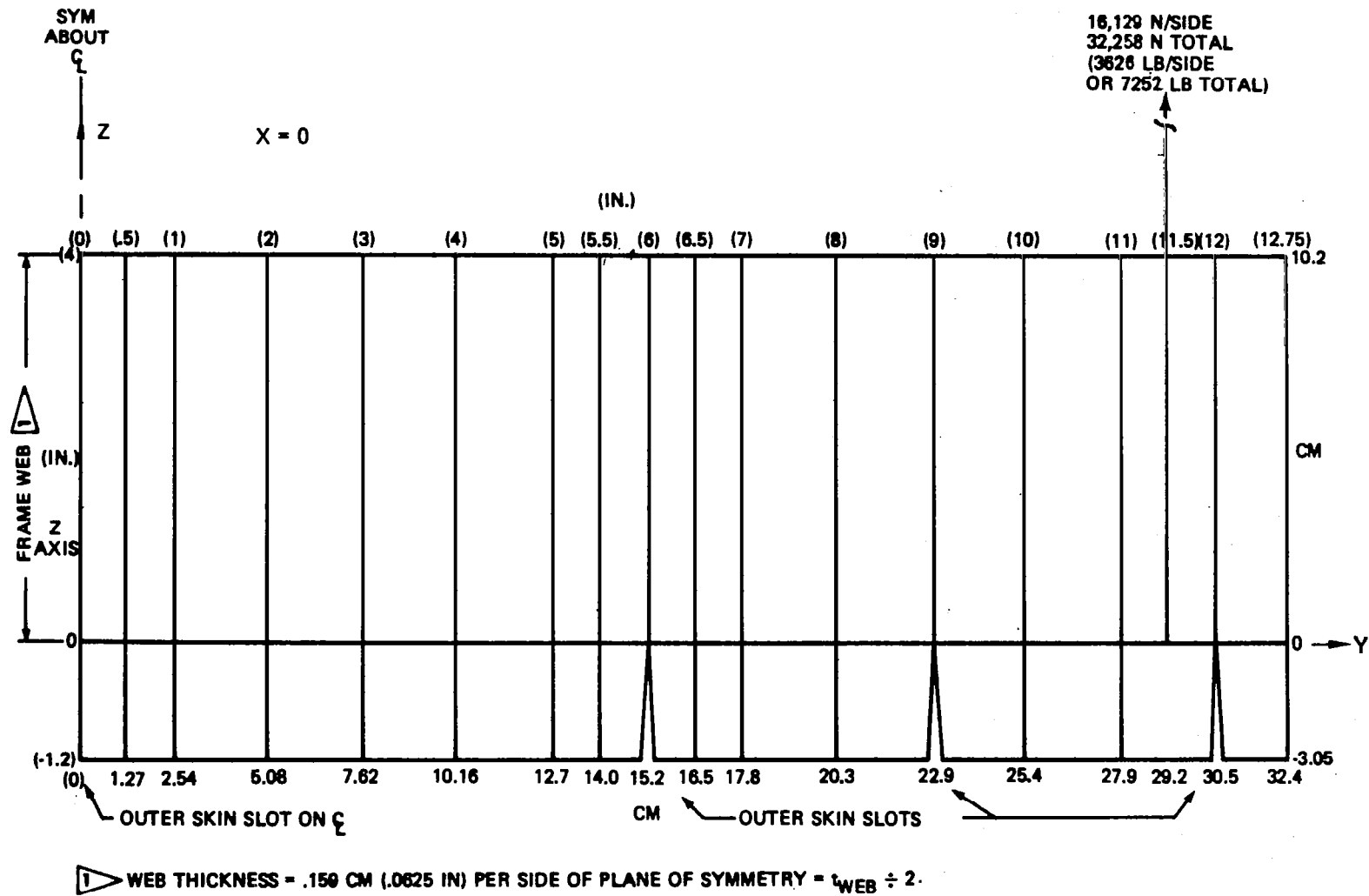


Figure A-8. Specimen 1 Finite Element Model Frame & Core Z & Y Coordinates

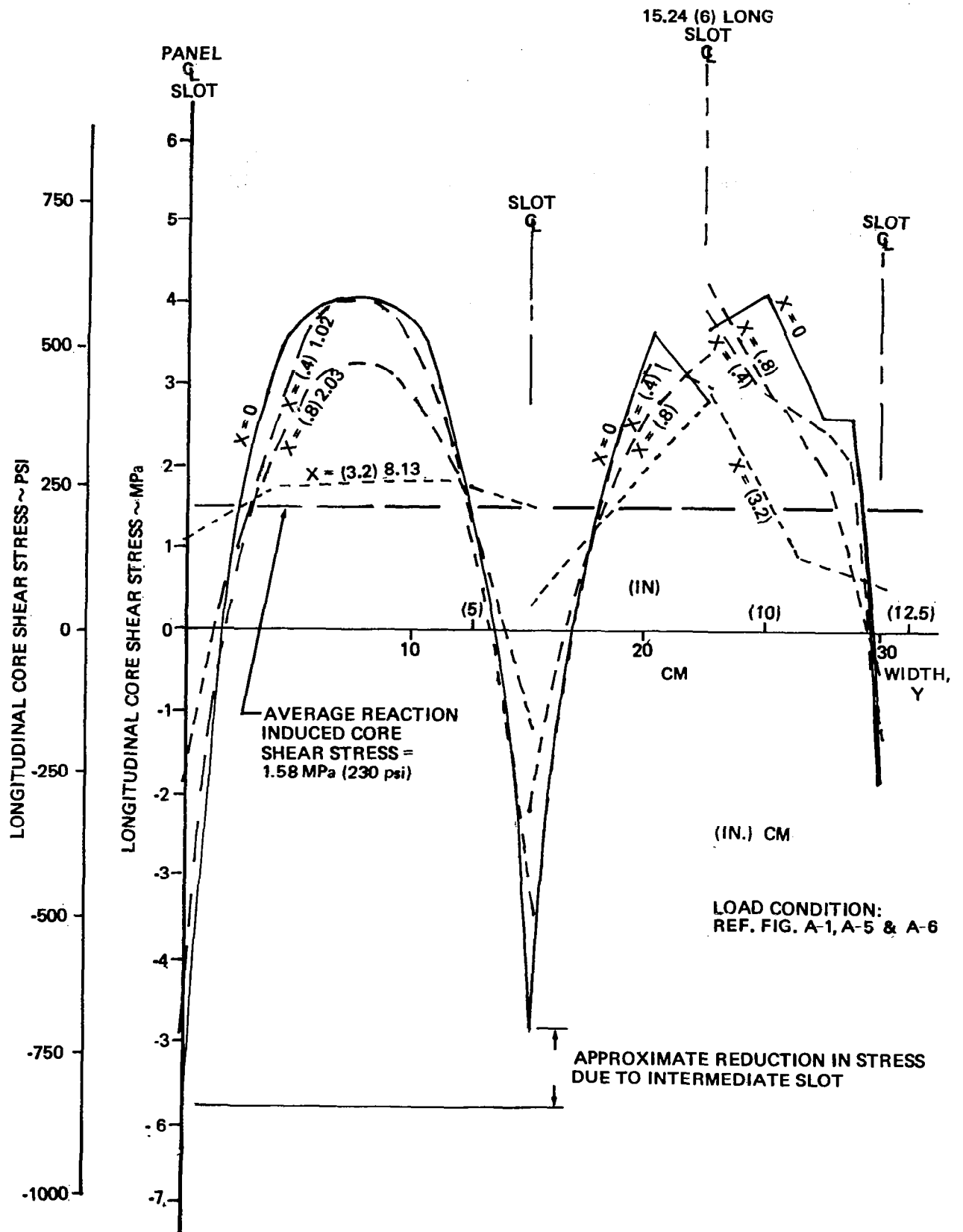


Figure A-9. Specimen 1 FEM Longitudinal Core Shear Stresses

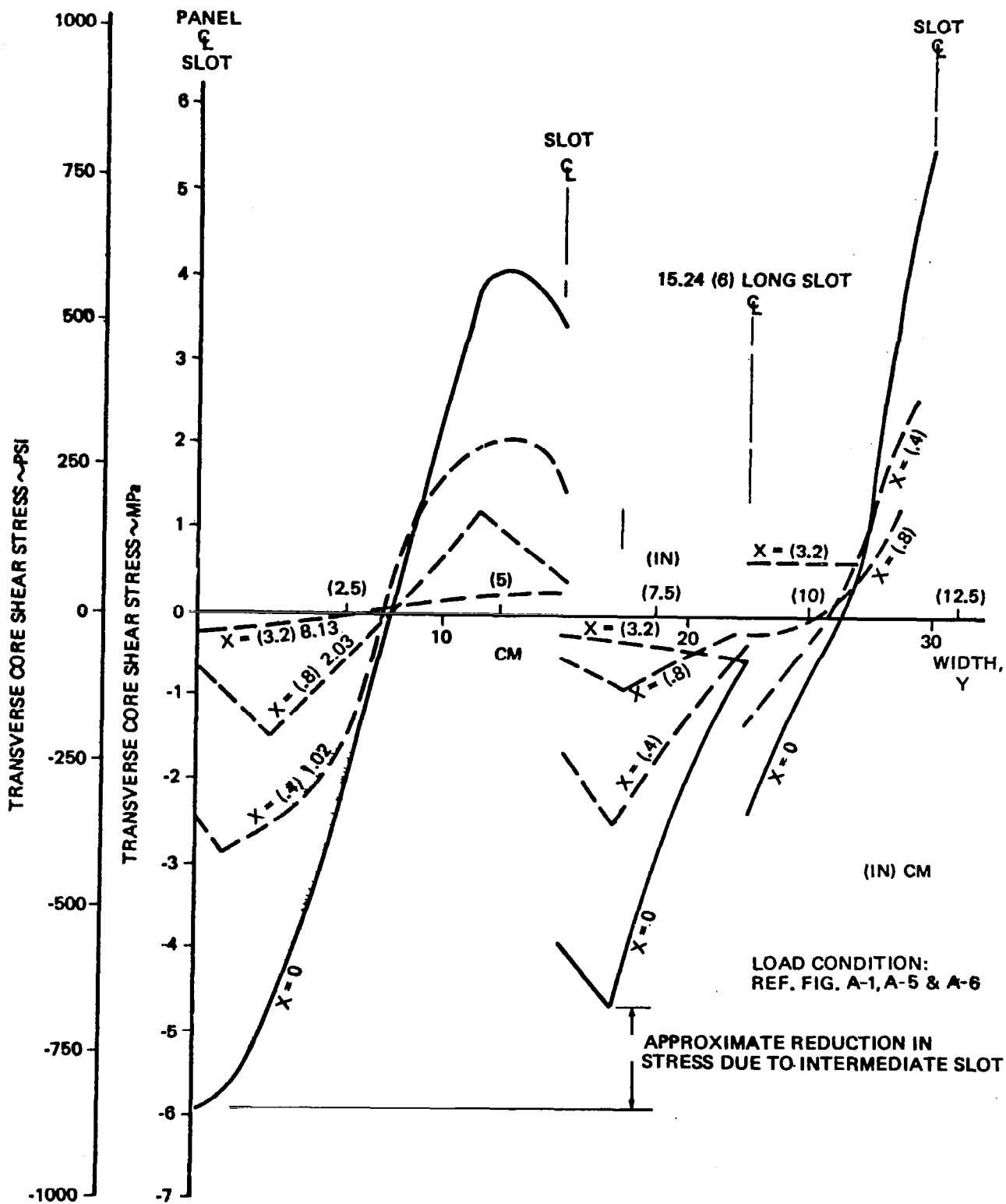


Figure A-10. Specimen 1 Transverse Core Shear Stresses

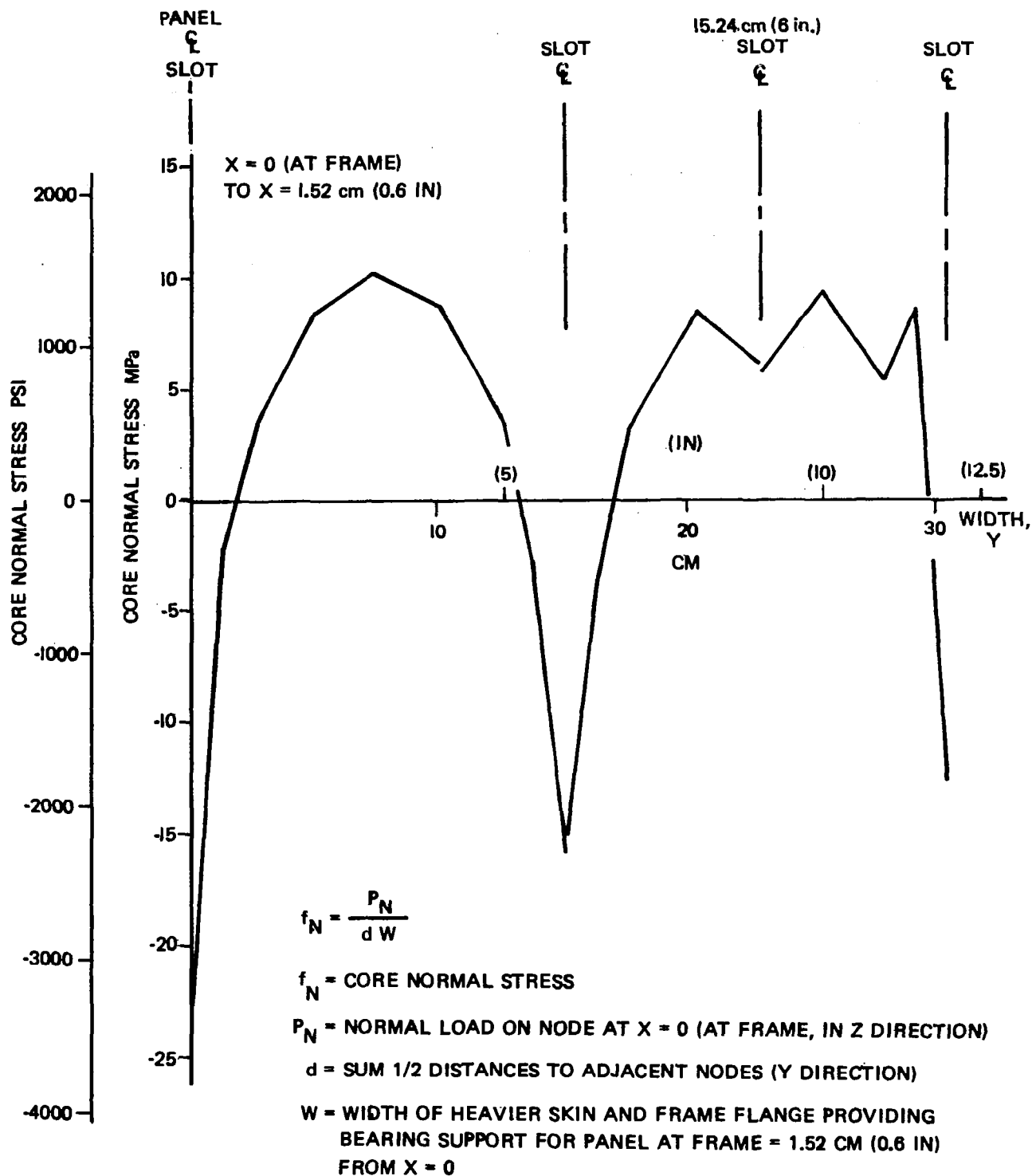


Figure A-11. Specimen 1 Core Normal Stresses at Frame Due to Thermal Loads.

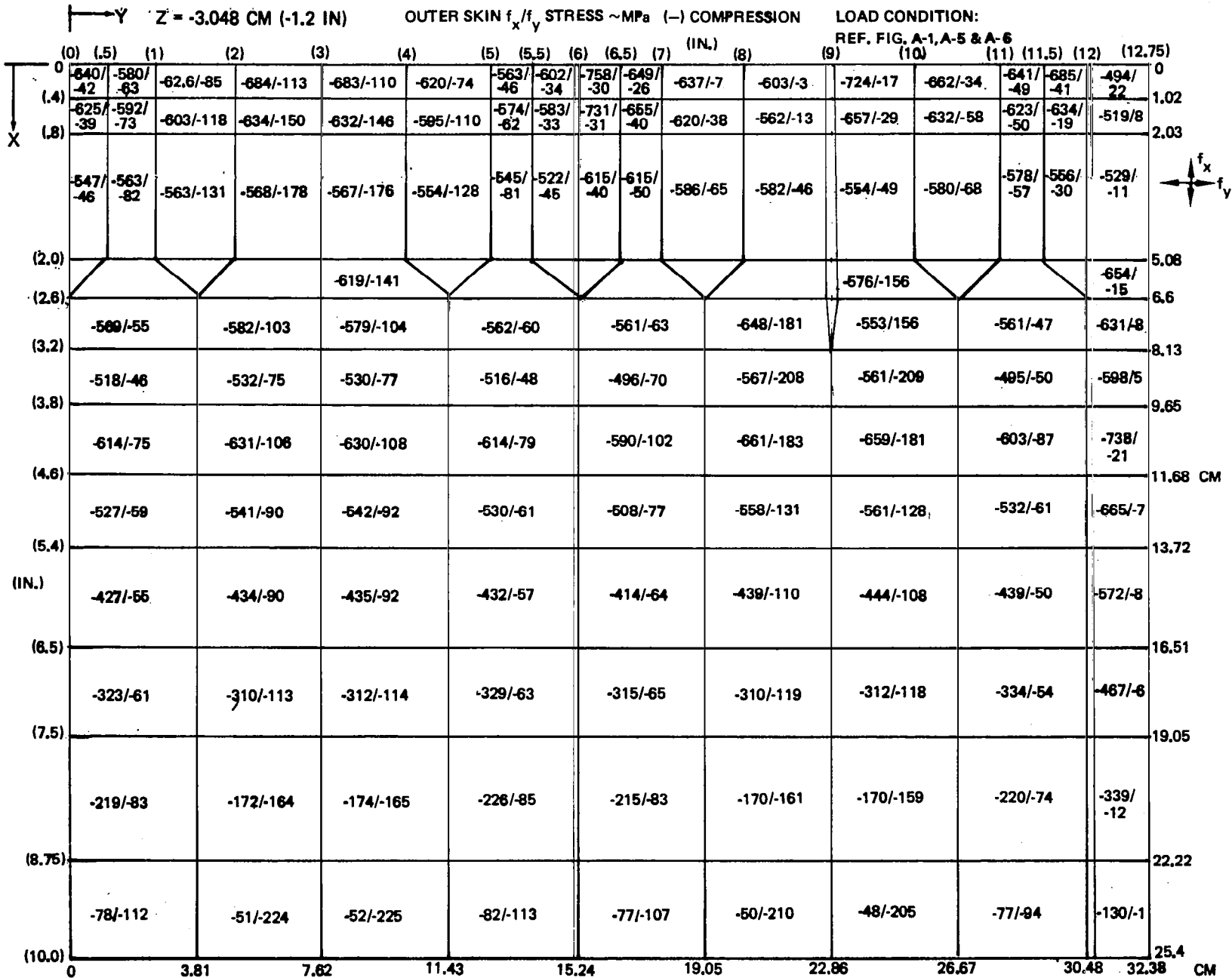


Figure A-12. Specimen 1 Outer Skin Inplane Stresses

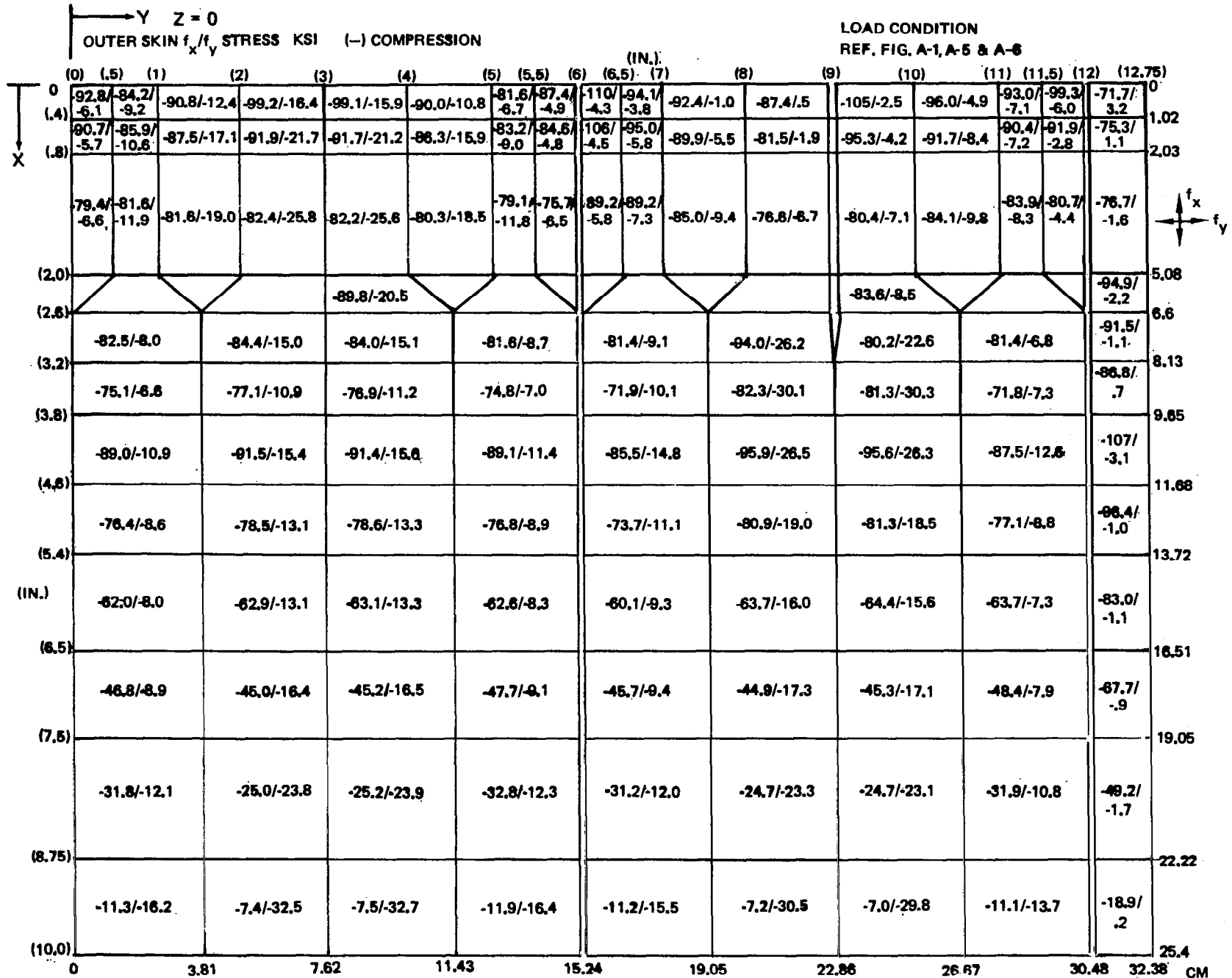


Figure A-13. Specimen 1 Outer Skin Inplane Stresses

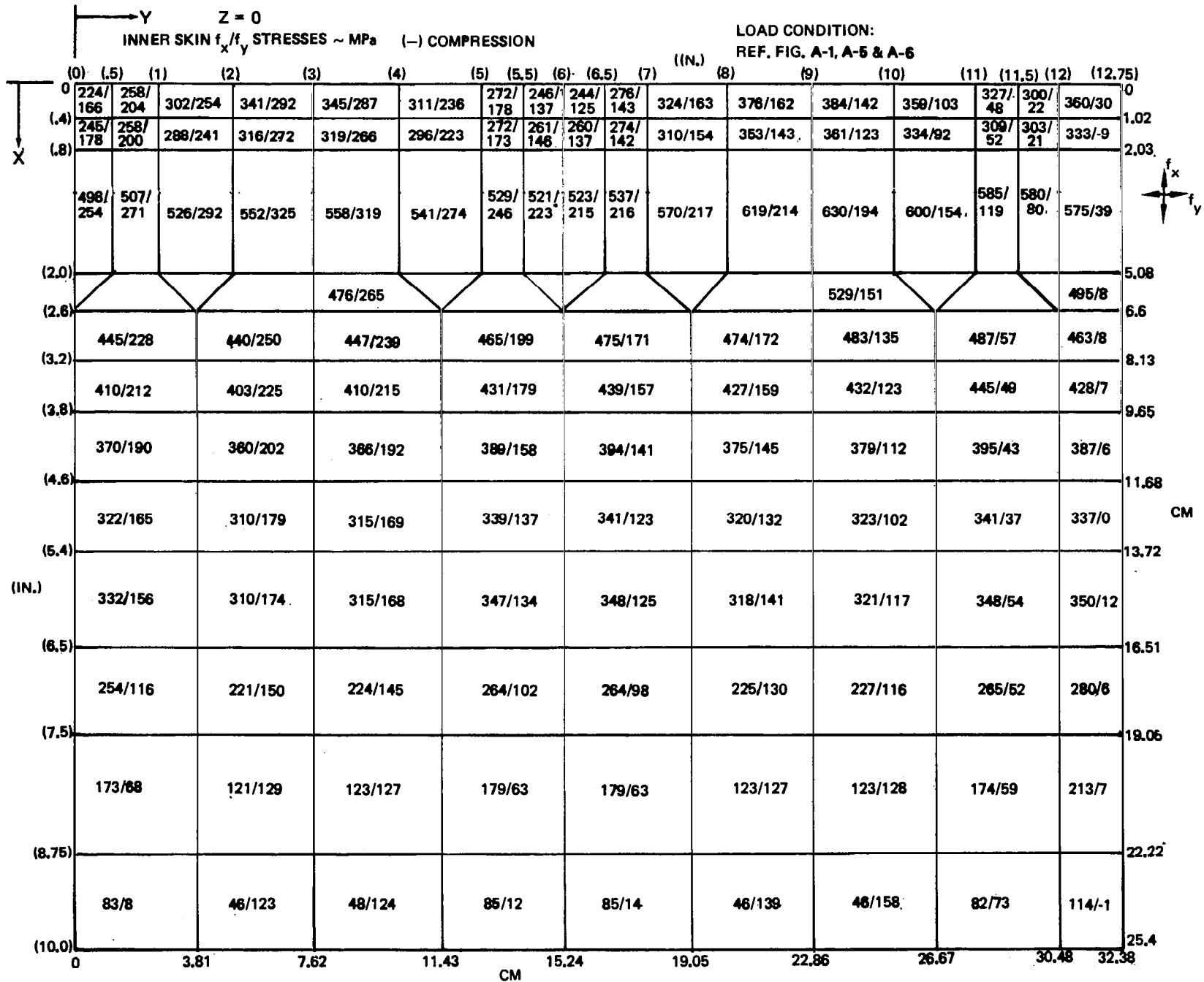


Figure A-14. Specimen 1 Inner Skin Inplane Stresses

INNER SKIN f_x/f_y STRESSES ~ KSI (-) COMPRESSION.

LOAD CONDITION:
REF. FIG. A-1, A-5 & A-6

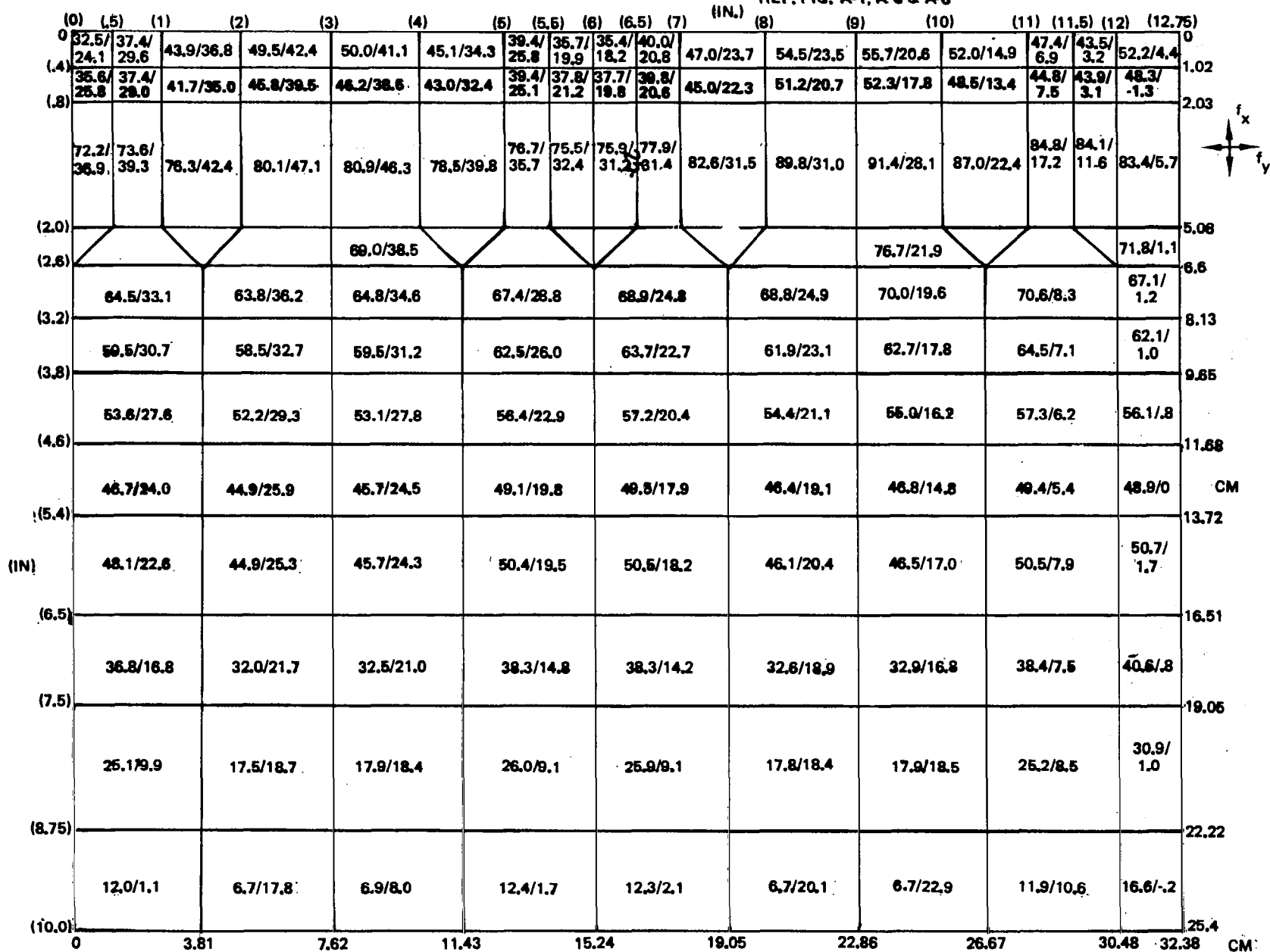


Figure A-15. Specimen 1 Inner Skin Inplane Stresses

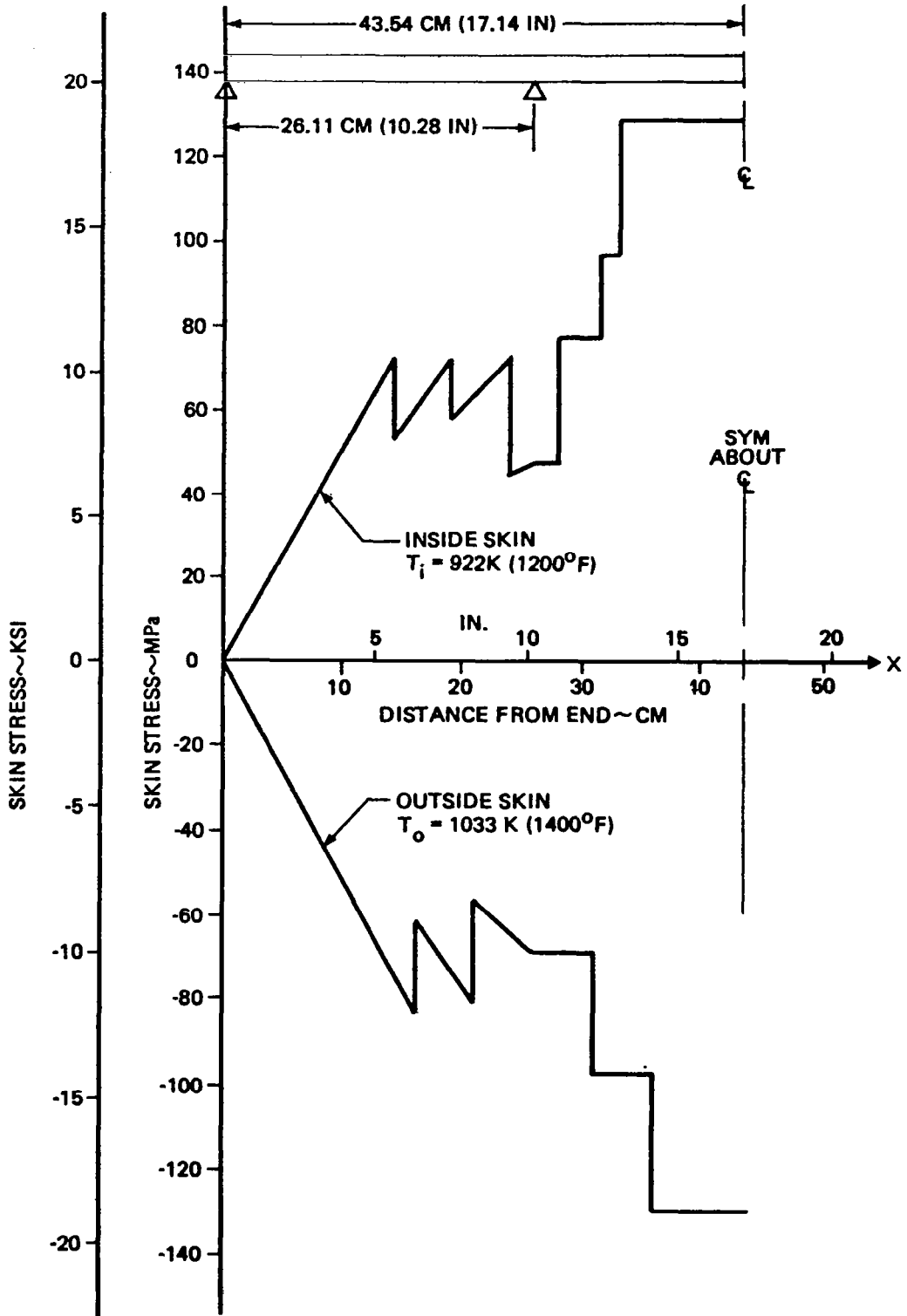


Figure A-16. Specimen 2 HTST Test Average Skin Stresses
See Figure A-2 for Load Condition

APPENDIX B

TEST LOG

Appendix B

TEST LOG

This appendix contains a condensation of the Specimen 1 test log.

10/14/80 10:00 Pressure built up to 5 psig in LH₂ dewar.
10:15 System is purged.
10:25 LH₂ fill begins.
Data is recorded every two minutes.
10:40 Vapor is visible out the vent stack and recording rate is switched to 30 sec.
10:50 First liquid level light is on and time lapse camera is turned on.
11:00 Cryostat is filled to a depth of 45.7 cm (18 in.)
11:11 Begin first thermal cycle.
11:20 Start real time camera.
11:56 It is noted that the first cycle induced temperatures above the desired 478K (400⁰F) on the panel (in fact as high as 683K (770⁰F). Frost over the controlling T/C is believed to be the cause. The controlling T/C is switched to T/C 3.
12:09 Start of second thermal cycle. The heat portion of the cycle is taken in steps to ensure that no part of the panel goes above 478K (400⁰F). It is decided that the control thermocouple will be programmed to ramp to 450K (350⁰F).
12:19 Lights off and hold begins. It takes longer than anticipated for the panel to cool as determined by the strip chart readings.
12:47 Start 3rd cycle.
1:32 Start 4th cycle.
2:20 Start 5th cycle.

- 3:08 Start 6th cycle.
- 3:12 Start hold for 6th cycle and monitor surface temperatures on strip chart.

TEMP (T/C 18) TIME

K	(^o F)	Min.
316	(+ 110)	5
286	(55)	10
277	(40)	15
269	(25)	20
255	(0)	30

- 3:45 Start 7th cycle. After this the surface temperatures are monitored with the data logger and found to reach (-200^oF) in less than three minutes. It is decided to shorten the hold period from 40 minutes to five.
- 4:06 Start 8th cycle.
- 4:27 Start 9th cycle.
- 4:38 Start 50 min. hold period. Recording rate switched to five minutes.
- 5:34 Recording rate switched to one minute and time lapse camera is started.
- 5:38 Start 10th cycle. Stopped to allow LH₂ fill.
- 5:47 Lights off.
- 6:04 Start container purge.

7:45 Purge complete. Inspection occurs. Time lapse camera is turned off. Some cracks are found in the foam insulation surrounding the LH₂ container. The lights look good and the Rene'41 panel is unchanged in appearance from the start of the test.

8:15 Purge begins.

8:30 LH₂ fill begins and time lapse camera is turned on.

9:13 Start cycle 11.

9:34 Start cycle 12. Lights malfunction.

9:50 Lamp controller reprogrammed, cycle 12 started.

10:11 Start cycle 13.

10:31 Start cycle 14.

10:52 Start cycle 15.

11:13 Start cycle 16.

11:33 Start cycle 17.

11:54 Start cycle 18.

10/15/80 12:14 Start cycle 19.

12:24 Begin 1 hour hold.

1:26 Start of cycle 20. Cycle 20 is followed by a 20 minute hold at 394K (250⁰F) in an attempt to remove frost from the panel surface. The hold has little visible effect on the frost.

1:51 Start cycle 21.

2:24 Start cycle 22.

2:42 Start cycle 23.

3:04 Start cycle 24.

3:25 Start cycle 25.

3:50 Start cycle 26.

4:06 Start cycle 27.

4:26 Start cycle 28.

4:47 Start cycle 29 and perform 50 minute hold.

5:47 Start cycle 30.

6:04 Start purge.

9:00 Inspection occurs. The test panel surface appearance is unchanged from before the start of test. Some cracks apparent in insulation around LH₂ container. LN₂ dewar reference junction is refilled. He supply is recharged.

9:50 Purge begins.

10:03 Time lapse camera is on. Fill begins.

10:12 Three (3) frost spots are visible on the foam on the container side.

10:29 Fill is complete.

10:36 Start cycle 31.

10:56 Start cycle 32.

11:17 Start cycle 33.

11:38 Start cycle 34. Three frost spots are gone.

12:00 Start cycle 35. NOTICE: The strip chart outside thermocouple (T/C 14) cycles are dropping to less cool (warmer) temperatures as cycles pass.

12:18 Start cycle 36.

12:30 Mild explosion? and fire. LH₂ supply is cut off and purge begun.

1:40 Container is warmed and inspected.

1:47 Area determined safe and observers allowed access. The container is burned on all sides with the side away from the camera burned the worst. Some of the bungee cord lashings burned through, releasing the bungee cords.

2:35 Running a heat only cycle. Real time camera turned on.

3:10 Area is returned to safe standby condition.

10/16/80

Photos were taken of the container. The lid was removed and pictures taken of the lid and inside of the container. The bolt nearest the inside patch (on the left when viewed from the camera position) was 1/8 turn looser than when installed. The other bolt was as installed.

Fiberfrax bearing pads look good and were in original position.

Center stiffener shows no signs of wear, yielding or failure.

Inside, GE RTV 102 Silicon Rubber Sealant patch material is still in place on a 25.24 cm (10 in.) run of panel to Hastelloy X seal weld (See Figure 14). The sealant is not cracked and generally in the same condition as when applied. Inside T/C exit hold plug is cracked (plug is silicon cement).

The silicon placed between the upper container flange and the lid is cracked and is burned in places. Photos were taken.

Fiberfrax bearing pad: Inside edge is darker (inside edge is side toward the stiffener).

There is a dark spot on the reflector below the spot where some foam (between the panel and container) was exposed.

When the lid was removed, water ran from between the lid and its foam covering.

Instrumentation engineer visually inspected the strain gages and noted appearance as normal.

10/17/80 The foam was removed from the container and lid to prepare for leak check.

The entire top is burned between the foam and lid. Removal was easy in that the top foam was already separated from the lid. Deposits of test fixture foam insulation were noted in the test panel outer skin open slots for approximately 1.27 cm (.5 in.) from the edge of the test panel. Test fixture Side 3 had the most burn.

Leak check - can find no leaks.

The bottom is cut free and the panel and brace examined. Both appear to be in excellent condition. The inside skin of the Rene'41 panel has a light gray appearance.

The position of the fiberfrax bearing pads can be seen on the test setup support frame flange by the slight difference in surface cast and was measured from the flange edge.

1. Report No. Report NASA CR-3525		2. Government Accession No.		3. Recipient's Catalog No.	
4. Title and Subtitle Cryogenic Performance of Slotted Brazen René 41 Honeycomb Panels				5. Report Date June 1982	
				6. Performing Organization Code	
7. Author(s) Andrew K. Hepler and Allan R. Swegle				8. Performing Organization Report No. D180-26653-1	
				10. Work Unit No.	
9. Performing Organization Name and Address Boeing Aerospace Company Kent, Washington 98031				11. Contract or Grant No. NAS1-14213	
				13. Type of Report and Period Covered Contractor Report - Final - Task V	
12. Sponsoring Agency Name and Address National Aeronautics and Space Administration Washington, D. C. 20546				14. Sponsoring Agency Code	
15. Supplementary Notes Langley Technical Monitor: John L. Shideler					
16. Abstract The objective of this program was to design, fabricate and test two brazen René'41 honeycomb panels that would incorporate a frame element. The panels were representative of the lower surface of an advanced space transportation vehicle. The first panel was a two span panel supported by a center frame and on edges parallel to it. The panel was 64.8 cm (25.5 IN) X 50.80 cm (20 IN) X 3.05 cm (1.2 IN) deep. The second panel was a three span panel supported on two frames and on edges parallel to the frames. The second panel was 56.6 cm (22.3 IN) X 87.1 cm (34.3 IN) X 3.048 cm (1.2 IN) deep. Each panel had its outer skin slotted to reduce the thermal stresses of the panel skins. The first panel was tested under simulated boost conditions that included liquid hydrogen exposure of the frame and inner skin and radiant heat to 478K (400°F) on the outer skins. The first panel was tested to investigate the effect of thermal stresses in skins and core caused by the panel being restrained by a cold integral frame and to observe the effects of frost formation and possible liquid air development in and around outer skin slots. The panel successfully completed 36 boost cycles. The second panel is to be subjected to hypersonic flow to an outer skin temperature of 1034K (1400°F) to simulate entry conditions. The second panel will be tested to evaluate the effects of hypersonic flow on covered and uncovered slots in the outer skin.					
17. Key Words (Suggested by Author(s)) Brazen Honeycomb Sandwich René'41 Advanced Space Transportation Thermal Stress Hot Structures			18. Distribution Statement Unclassified - Unlimited Star Category 39		
19. Security Classif. (of this report) Unclassified		20. Security Classif. (of this page) Unclassified		21. No. of Pages 92	22. Price A05